

ASSESSING THE WATER QUALITY OF THE SAZLIDERE RESERVOIR IN ISTANBUL WITH IKONOS SATELLITE IMAGERY

Thesis submitted to the

Institute of Social Sciences

in partial fulfillment of the requirements

for the degree of

Master of Arts

in

Geography

by

Aysel SHAMIS

Fatih University

June 2010

© Aysel SHAMIS

All Rights Reserved, 2010

APPROVAL PAGE

Student : Aysel SHAMIS
Institute : Institute of Social Sciences
Department : Geography
Thesis Subject : Assessing the Water Quality of the Sazlıdere Reservoir in
Istanbul with IKONOS Satellite Imagery
Thesis Date : June 2010

I certify that this thesis satisfies all the requirements as a thesis for the degree of Master of Arts.

Assoc. Prof. Ali DEMİRCİ
Head of Department

This is to certify that I have read this thesis and that in my opinion it is fully adequate, in scope and quality, as a thesis for the degree of Master of Arts.

Assist. Prof.Dr. Ahmet KARABURUN
Supervisor

Examining Committee Members

Assist. Prof. Dr. Ahmet KARABURUN

Assist. Prof. Dr. Süleyman İNCEKARA

Assist. Prof. Dr. Ferhat KARACA

It is approved that this thesis has been written in compliance with the formatting rules laid down by the Graduate Institute of Social Sciences.

Assoc. Prof. Mehmet KARAKUYU
Director

AUTHOR DECLARATIONS

1. The material included in this thesis has not been submitted wholly or in part for any academic award or qualification other than that for which it is now submitted.
2. The program of advanced study of which this thesis is part has consisted of:
 - i) A Research Methods course during undergraduate study
 - ii) An examination of several thesis guides of particular universities both in Turkey and abroad as well as a professional book on this subject.

Aysel SHAMIS

June, 2010

ABSTRACT

AYSEL SHAMIS

JUNE 2010

ASSESSING THE WATER QUALITY OF THE SAZLIDERE RESERVOIR IN ISTANBUL WITH IKONOS SATELLITE IMAGERY

Eutrophication and sediment related problems threaten the water quality of lakes and reservoirs that supply public drinking water. Population growth and land developments have increased considerations about the safe supply of water, especially in urban areas. Since most of the watersheds draining into water supply reservoirs contain mixed land uses, consisting of urban, residential, industrial and agricultural areas, water resource areas have received an increased level of pollutants coming from the surrounding area. Thus the protection and management of drinking water sources and their watershed areas have become increasingly important. The use of satellite data has been proven to be useful in terms of water quality monitoring and assessment. Due to its capability of providing high spatial details and synoptic views of the water quality parameters, distributions and watershed characteristics, high resolution satellite data enables valuable information in the assessments of water quality covering an entire water body.

The goal of this study is to use satellite-derived data for assessing water quality with respect to the trophic condition and suspended sediment concentrations in the Sazlıdere reservoir, which is based on quantifying and mapping the distribution of quality indicators (suspended sediment, chlorophyll-a, total phosphate, secchi disc depth). IKONOS imagery was used to obtain satellite-based information for investigating the spatial and temporal variations in water quality indicators and their controlling factors to clarify dynamics in the Sazlıdere reservoir. Thematic maps from satellite imagery were produced by predictive empirical models through statistical analysis of the relationship between water quality parameters and their corresponding atmospherically corrected IKONOS data. Satellite-derived data have provided valuable information in the assessments of water quality covering temporally and spatially the entire water body of the reservoir. The results indicated that the effects of climate on the reservoir's water level were important factors affecting water quality. Providing high spatial coverage and clear visual differentiation between the patterns of distribution of water quality parameters, satellite data has been demonstrated to have potential for use as a guide for designing and improving methods for finding the best locations to carry out ground sampling.

Key words:

Satellite Images, IKONOS, Thematic maps, Water Quality Monitoring and Assessment

KISA ÖZET

AYSEL SHAMIS

HAZİRAN 2010

IKONOS UYDU VERİSİYLE SAZLIDERE REZARVUARININ SU KALİTESİNİN DEĞERLENDİRİLMESİ

Günümüzde ötrofikasyon ve sediment kaynaklı sorunlar içme suyu sağlayan göl ve rezervuarların su kalitesini tehdit etmektedir. Nüfus artışı ve alansal büyüme özellikle kentsel alanlarda güvenli su sağlama konusundaki endişeleri artırmıştır. İçme suyu sağlayan rezervuarları besleyen havzaların çoğu kent, konut, sanayi ve tarım alanlardan meydana gelen karma bir arazi kullanımı içerdiğinden su kaynakları, çevresindeki bu alanlardan artan düzeyde kirleticiler almaktadır. Bu yüzden içme suyu kaynakları ve onların havza alanlarının korunması ve yönetimi giderek daha da önemli hale gelmiştir. Uydu verilerinin su kalitesi izleme ve değerlendirme açısından yararlılığı kanıtlanmış durumdadır. Su kalitesi parametrelerinin dağılımları ve havza özellikleri için sağladığı yüksek alansal detay ve sinoptik görüş yeteneği nedeniyle yüksek çözünürlüklü uydu verileri, bütün rezervuar alanını içeren su kalitesi değerlendirmesine katkıda bulunmaktadır.

Bu çalışmanın amacı, Sazlıdere rezervuarındaki trofik duruma ve askıdaki sedimentlerin yoğunluğuna göre yapılan su kalite değerlendirilmesi için su kalitesi göstergelerinin (askıda sediment, klorofil, toplam fosfat, sechi disk) dağılımının sayısallaştırılması ve haritalanması temeline dayanan uydu kaynaklı veri kullanmaktır. IKONOS görüntüleri Sazlıdere rezervuarının dinamizmini belirlemek için su kalitesi göstergelerindeki alansal ve zamansal değişimlerin ve bunların kontrol etmenlerinin araştırılmasında uydu tabanlı bilgi edinmede kullanılmıştır. Uydu görüntülerinden elde edilen tematik haritalar, kestirimci ampirik modeller tarafından su kalite parametreleri ve bunlara karşılık gelen atmosferik olarak düzeltilmiş olan IKONOS verileri arasındaki ilişkinin istatistiksel analizi yoluyla üretilmiştir. Uydu kaynaklı veri zamansal ve alansal olarak rezervuardaki su alanını bütünü için yapılan su kalitesi değerlendirmesinde faydalı bilgiler sağlamıştır. Sonuçlar, rezervuar su seviyesi üzerinde iklimin etkisinin su kalitesini etkileyen önemli faktör olduğunu göstermiştir. Ayrıca su kalitesi parametrelerinin dağılım şablonunda alansal kapsama ve açık görsel ayrışma sağlamasıyla Uzaktan Algılama, arazi su örnekleme uygulaması için en iyi noktaları belirlemeyi dizayn etmede ve geliştirilmesine rehberlik sağlamada büyük bir potansiyele sahip olduğunu göstermiştir.

Anahtar Kelimeler:

Uydu Görüntüleri, IKONOS, Tematik Haritalar, Su Kalitesinin İzlenmesi ve Değerlendirilmesi.

LIST OF CONTENTS

APPROVAL PAGE.....	iii
ABSTRACT.....	v
KISA ÖZET.....	vi
LIST OF TABLES.....	x
LIST OF FIGURES.....	xi
LIST OF APPENDICES.....	xiii
LIST OF ABBREVIATIONS.....	xiv
ACKNOWLEDGEMENTS.....	xv
CHAPTER 1.....	1
INTRODUCTION.....	1
1.1 Background.....	1
1.2 Study Area.....	7
1.3 Hypothesis and Purpose of Study.....	8
1.4 Benefits of the Research.....	9
1.5 Thesis Structural Organization.....	11
CHAPTER 2.....	12
LITERATURE REVIEW.....	12
2.1 Introduction.....	12
2.2 Remote Sensing Technology and Water Quality Applications.....	12
2.3 High Spatial Resolution Imagery and IKONOS.....	14
2.4 Image Preprocessing.....	16
2.4.1 Radiometric Normalization.....	17
2.4.2 Atmospheric Correction.....	18
2.4.2.1 Atmospheric Correction in ATCOR.....	20
2.5 Development of Water Quality Parameters through the Remote Sensing Method.....	23
2.5.1 Empirical Approach.....	26
2.6 Assessing Water Quality Parameters.....	28

2.6.1 Carlson Trophic-State Index.....	28
CHAPTER 3.....	31
THE PHYSICAL ENVIRONMENT AND LAND USE OF THE SAZLIDERE WATERSHED.....	31
3.1 Introduction.....	31
3.2 Effects of Climate on Water quality.....	32
3.2.1 Temperature and Precipitation Characteristics in the Watershed.....	33
3.2.2 Water Level Changes in the Reservoir.....	40
3.2.3 The characteristics of winds in the watershed.....	42
3.3 Land Use and Water quality.....	45
3.3.1 Land Uses in the Watershed.....	46
3.4 Topography.....	49
3.5 Geology.....	51
3.6 Soil.....	53
3.6.1 Water Erosion.....	55
CHAPTER 4.....	57
MATERIALS AND METHODOLOGY.....	57
4.1 Introduction.....	57
4.2 Data Collection.....	57
4.2.1 Satellite Data.....	58
4.2.2 Ground Observation Data.....	58
4.2.3 Atmospheric Data.....	59
4.3 Image Preprocessing.....	60
4.3.1 Atmospheric Correction.....	60
4.4 Extraction of Reservoir Water Image.....	64
4.5 Derivation of Water Spectral Signatures.....	64
4.6 Multiple Regression Analysis and its Validation Using Jackknife Resampling....	65
4.7 Water Quality Maps.....	67
CHAPTER 5.....	68
RESULTS AND CONCLUSIONS.....	68

5.1 Introduction.....	68
5.2 Results and Discussions.....	69
5.2.1 Regression Analysis.....	69
5.2.2 Spatial and Temporal Variations of Water Quality Parameters	70
5.2.3 Land use and water quality.....	76
5.3 Conclusions.....	76
5.3.1 Limitations of the Study.....	79
5.3.2 Future research.....	80
APPENDICES	82
BIBLIOGRAPHY.....	94

LIST OF TABLES

TABLE 1: TROPHIC STATE INDEX (Carlson and Simpson, 1996).....	29
TABLE 2: THE PREVAILING WIND DIRECTION (1975-2008)	42
TABLE 3: THE PREVAILING WIND DIRECTION (2007 - 2008)	42
TABLE 4: MAXIMUM WIND SPEED AND ITS DIRECTION (2007 - 2008)	43
TABLE 5: SATELLITE DATA USED IN THIS STUDY	58
TABLE 6 : INFORMATION FOR GROUND OBSERVATION DATA	59

LIST OF FIGURES

Figure 1: The location of the Sazlıdere reservoir (study area) and its watershed.	8
Figure 2: The relationship between reflectance and the electromagnetic spectrum for increased suspended sediment (Ritchie and Cooper, 2001).....	24
Figure 3: Reflectance across most wavelengths with increased chlorophyll concentration (Ritchie and Cooper, 2001).	25
Figure 4: Total annual precipitation in the Çatalca, Florya and Bahçeköy Meteorological Stations between 1975 and 2008.....	34
Figure 5: Average Temperature of the Çatalca, Florya and Bahçeköy Meteorological Stations between 1975 and 2008	35
Figure 6: Comparison of the average monthly precipitation between 2007 and 1975-2008 (Florya Meteorological Station).....	36
Figure 7: Comparison of the average monthly precipitation between 2007 and 1975-2008 (Florya Meteorological Station).....	37
Figure 8: The total seasonal precipitation in 2007, 2008 and 1975-2008 (Florya Meteorological Station).....	38
Figure 9: Comparison of the average monthly temperature between 2007 and 1975-2008 (Florya Meteorological Station).....	39
Figure 10: Comparison of the average monthly temperature between 2007 and 1975-2008 (Florya Meteorological Station).....	39
Figure 11: The amount of runoff discharged into the water supply reservoirs in Istanbul from 2001 to 2008 (www.iski.gov.tr accessed May 30, 2010).....	40
Figure 12: The percent filled to capacity of Istanbul water supply dams on May 30 from 2001 to 2008. (www.iski.gov.tr accessed May 30, 2010).	41

Figure 13: Land use map of the watershed	47
Figure 14: The slope map of the watershed.	50
Figure 15: Geological map of the Sazlıdere catchment area (produced from the original Geological Map of Turkey, General Directorate of Mineral Research and Exploration, 2002).	52
Figure 16: Soil map of the Sazlıdere watershed (taken from the General Directorate of Agricultural Research).	54
Figure 17: Map showing the degree of water erosion (taken from the General Directorate of Agricultural Research).	56
Figure 18: The distribution of Chl-a concentration in 2007 - 2008.	72
Figure 19: The distribution of TP concentration in 2007 - 2008.	73
Figure 20: The distribution of TSS concentration in 2007 – 2008.	74
Figure 21: The distribution of turbidity (SDT) in 2007 and 2008.	75

LIST OF APPENDICES

Appendix 1: IKONOS Image Metadata (2007 -2008).....	82
Appendix 2: Atcor Inputs for IKONOS Image (2007-2008).....	83
Appendix 3: IKONOS Bands Used in the Regression Analysis (2007-2008).....	84
Appendix 4: Ground Reference Measurements Used in the Regression Analysis (2007-2008).....	84
Appendix 5: Regression Models and their Coefficient of Determination $s(R^2)$, and Models Performances based on Jackknife resampling method (2007-2008).....	85
Appendix 6: Coefficients of Linear Regression Models and Jackknife Sampling Estimates of the Regression Coefficients, and Biases (2007-2008).....	87
Appendix 7: Water Quality Parameter Model Performances based on the Jackknife Resampling Method (2007-2008).....	90

LIST OF ABBREVIATIONS

Chl-a	Choloropll a
DN	Digital Number
LUTs	Look-up Tables
MODTRAN	Moderate Spectral Resolution Atmospheric Transmission Model
NASA	National Aeronautics and Space Administration
RMSE	Root Mean Square Error
RTM	Radiative Transfer Model
SDT	Secchi Disc Transparency
TAO	Top of Atmosphere
TP	Total Phosphate
TSI	Trophic-State Index
TSS	Total Suspended Solids
UTM	Universal Transversal Mercator

ACKNOWLEDGEMENTS

I would like to thank those at Fatih University who helped me to complete this thesis: Ahmet Karaburun, Ferhat Karaca and Süleyman Incekara. I would also like to thank Michael Andy McAdams, who helped me get started on this project, Ali Demirci, who gave me advice on how to finish the project, and Mehmet Karakuyu. Those from ISKI's map department who helped me greatly were Mustafa Oğurlu, Ayşe Özkan, Filiz Demirci and Ünal Kartal. Ömer Visalı Sarıkaya's help with the technical part of my thesis was indispensable. Also, thanks is due to Cihangir Aydöner from TUBITAK. I would like to thank Rahime Günay and Sevim Ünügür for their continual encouragement and support. Lastly, I would like to thank Matthew Shamis, who edited my thesis, Joseph Shamis, and the rest of my family in America and Turkey for their continual support.

CHAPTER 1

INTRODUCTION

1.1 Background

In an undisturbed environment, nutrients and sediment loading into aquatic systems occurs gradually as a natural process. With undisturbed conditions, very few aquatic systems experience eutrophic waters (Prepas and Charette, 2003) and sediment infilling may occur particularly in shallow systems. The natural processes that occur in bodies of water can be accelerated by an excess of nutrient and sediment inputs from human activities. Anthropogenic nutrient enrichment leads to eutrophic conditions that cause the excessive and rapid growth of aquatic plants and algae which later can result in algal blooms. Increased sediment loading can cause deterioration of aquatic habitats.

Eutrophication and sediment related problems threaten the water quality of lakes or reservoirs that supply public drinking water. Both algal growth and fine sediments suspended in water can result in reduced water clarity. Eutrophic water can cause taste and odor problems, clog pipelines and cause an oxygen deficiency (Mueller and Helsel, 1996) which is important for biological life. Also it can contaminate water supplies with nitrate and algal toxic effects (Ironside, 2001) which threaten human health. Treatment of such eutrophic conditions for the drinking water supply can be difficult. On the other hand, sediment can cause a reduced storage capacity for water reservoirs, while contributing to algal growth by increasing nutrients carried in absorption form. Chemicals deposited in bottom sediment can be released with changes in water environmental conditions such as the development of anaerobic

processes and a decreasing water level. Treatment costs for sediment in water for drinking can increase.

Nutrients are the chemical elements that supply important nutrition to organisms (Ironside, 2001). While a certain amount of nutrients in water helps to support aquatic ecosystems, at high levels they can negatively affect the aquatic life and human health (Mueller and Helsel, 1996). Nitrogen and phosphorus are two nutrients that have a direct impact on water quality (De la Cretaz and Barten, 2007). Phosphorus levels have an effect on algae growth in fresh water, and likewise, nitrogen affects algae growth in ocean waters (Ironside, 2001).

Nutrients and sediment generally are introduced to water reservoirs through runoff from upstream land of watersheds. These constituents are carried to downstream reservoirs from agriculture, urban, and industrial, as well domestic sewage. The major phosphorus concentrations in surface water are released from agricultural and urban areas (Carpenter, 1998). Phosphates from commercial fertilizers applied in farming practices are important contributors to surface water contaminants (De la Cretaz and Barten, 2007). Septic wastewater system effluent is a potential source of phosphorus in surface water (Jones and Lee, 1979). Phosphorus from detergents containing phosphates is added to sewage systems (Brown, 2003). In winter, phosphorus loading is higher, while phosphorus concentrations in the summer are more likely to be caused by on-site changes. Eutrophication that occurs over a long period of time, and organic sedimentation which causes phosphorus enrichment may result in internal phosphorus loading (Prepas and Charette, 2003).

Population growth and land developments have increased considerations about the safe water supply especially in urban areas. Water pollution from increased surface

loadings from land, enlarged agricultural and industrial runoff, amplified municipal sewage, as well as expanded chemical technology can lead to serious problems. The protection and management of drinking water sources and their watershed areas have become greatly important.

In urbanizing areas, most of the watersheds draining into water supply reservoirs contain mixed land uses consisting of urban, residential, industrial and agricultural areas. Water resource areas receive pollutants resulting from urban and agricultural environments, permitted or unpermitted discharges of waste water, discharges of sewage systems, and urban air by depositing particles on the water's surface (Whipple, 1994). Uncontrolled or unregulated developments within watersheds can cause serious problems. For example, pollutants from the construction of houses and other facilities close to water or any activities beside water enter directly into water sources. The protection of watersheds and reservoirs from development pressures and urban growth often becomes difficult (Whipple, 1994). Conservation of entire watersheds as open spaces and habitats would be the best solution, but this practice is uneconomical for current conditions. Land development can be allowed in the case that land is provided for the protection of drinking water from pollutants (Whipple, 1994). Some problems related to water supply reservoirs caused by development within watersheds have occurred in the city of Istanbul, which is experiencing great pressure from population growth and rapid urbanization. Due to extensive and unregulated land development as well as no protective regulations in the watershed, the city has lost one of its water supply reservoirs (Demirci *et al.* 2006). In this sense, the monitoring and protection of water resources becomes an important issue for the city authority's water quality mission.

It is essential for water management authorities that they observe the continuing effect of land development and human activities on water quality, determine the constituents that affect water quality and ascertain if the water is good for its intended use. This is especially important for water resources that supply drinking water for a city. There are various parameters used to measure water quality. These parameters provide information about both the quality of water and the level of pollution. Sediment and eutrophication levels are measured by some key indicators. These are Total Suspended Solids (TSS), Secchi Disc Transparency (SDT), Chlorophyll-a (Chl-a), and Total Phosphate (TP).

TSS represents the turbidity or amount of solids suspended in the water such as soil particles, industrial waste, and sewage. However, the TSS is the measuring of a dry weight of material in a particular volume of water. TSS is generally used to calculate total concentrations of suspended solid-phase material in surface waters (Gray *et al.* 2000).

Secchi Disc is used to measure water clarity or turbidity by visual observation. It is usually referred to as Secchi Disc Depth or Transparency. Clarity can be affected by algae, soil particles, and other materials. Algae represent the most dominant effect on clarity of water (Fuller and Minnerick, 2007). Secchi Disk depth is largely used to demonstrate the biological productivity of a lake.

Chlorophyll-a is a common photosynthetic pigment found in all phytoplankton (e.g. algae). It is used to measure the density of the algal population (Fuller and Minnerick, 2007) and is a principal indicator of trophic level in a lake.

TP is the most analyzed fraction of phosphorus, which represents the total of all filterable and particulate phosphorus forms (Carlson and Simpson, 1996). It is used to represent the total amount of phosphorus in a lake.

The examination of the spatial distribution of quality parameters in water bodies and the monitoring of temporal changes in these parameters have been done using water sampling and laboratory analysis of the samples. Ground measurements basically depend on samples taken from specific locations in the water bodies. These samples provide information for the selected locations (Campbell, 2002) and are largely used in examining and monitoring variations in the distribution of quality parameters spatially over entire water bodies. At this point, remote sensing technology has become a potential supplement to ground measurements. Remote sensing technology, used along with modern computerized data processing, has offered promise for determining and mapping concentrations and distributions of quality parameters (suspended sediment, secchi disc depth, chlorophyll-a, total phosphate) over the entire water body. The synoptic view and revisit capability of satellite remote sensing allows for spatial and temporal monitoring of quality parameters and watershed characteristics over large areas and even in remote inaccessible areas. Methods for determining water quality parameters from satellite data depend on the coordination between ground and satellite measurements. Satellite based measurements consist of the energy reflected from physical variations of each water quality parameters over water bodies. Ground measurement data are used for reference data to calibrate quality parameters for the whole water surface with measurements obtained from the remote sensing technique. Satellite based estimates of water quality are usually obtained from the modeling of statistical

relationships between the spectral reflectance of water constituents(e.g. suspended sediment) and the corresponding ground measurements (Nellis *et al.* 1998).

Satellite data offers many potential uses including water quality assessment over large areas (e.g. regional scale),assessment of how watershed land use change affects water quality, and designing ground monitoring programs through selecting the best locations of sampling points (Dekker, 1993).

One advancement in remote sensing technology is the use of high spatial resolution of satellite (e.g. IKONOS) images to study water quality, which has contributed greatly to applying the quality of parameters for small lakes and understanding the impact of adjacent land use on the water quality (Sawaya *et al.* 2003).

Although remote sensing technology can contribute to various water quality measurements, it cannot by itself provide all water quality information required by water management agencies or authorities. The need of providing both ground and space monitoring systems has an impact on costs. It is very expensive to study water quality assessment over large areas with some satellite systems (e.g. IKONOS). Remote sensing may be used in various application areas and remote sensing technology can be made more affordable if data acquisition costs can be shared among municipal departments, government organizations and research centers (Bukata, 2005). For instance, IKONOS data, due to its high spatial resolution can be used for various applications, such as municipal transportation planning and the monitoring of forest conditions. Therefore each department can benefit from the implementation and sharing of satellite data.

1.2 Study Area

The study area (Figure 1), Sazlıdere reservoir, located in the west part of Istanbul, is one of its primary water resources. The reservoir was chosen as the study area for this research because of the availability of ground and satellite data with acquisition dates close to each other, which is recommended for satellite based water quality assessment (Olmanson *et al.* 2002).

Sazlıdere is a drinking water supply reservoir created by a dam made in 1998. The reservoir's drainage area covers around 165 square kilometers. Its water supply capacity is 91,600,000 m³/year. It supplies approximately 15 % of city water. The reservoir's surface area is about 11.8 km², with a maximum depth of about 21.6 m, and a mean depth of about 10.8 m (Istanbul Çevre ve Orman Müdürlüğü, 2005). The major streams which drain into the reservoir are Dursunköy, Boyalık, Baklalı, Derbent and Türköse (ISKI).

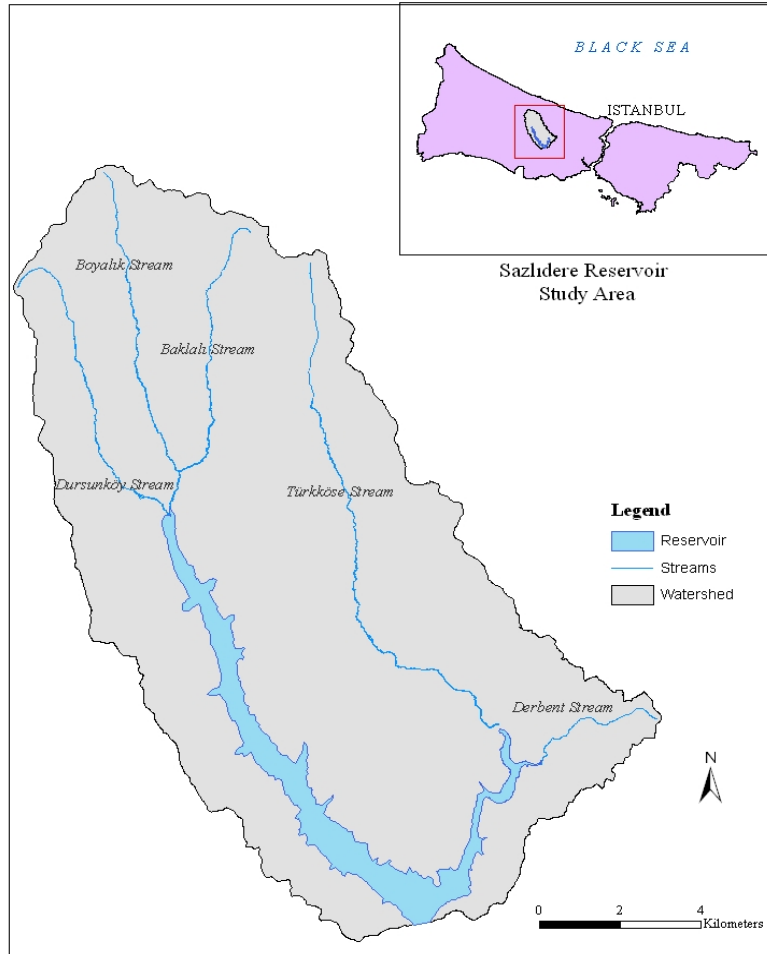


Figure 1: The location of the Sazlıdere reservoir (study area) and its watershed.

1.3 Hypothesis and Purpose of Study

It is hypothesized that water quality in the Sazlıdere reservoir can be assessed regarding trophic condition and sediment yield using IKONOS satellite imagery through quantifying and mapping distribution of quality indicators (suspended sediment, chlorophyll a, total phosphate, secchi disk). To this end, predictive models for water quality indicators were established based on statistical relationships between the reflectance value of each indicator in the satellite imagery and corresponding ground measurements. Thematic maps representing spatial patterns of

pollutant distribution were produced using the predictive models, and maps of reservoir productivity indicators were categorized according to the Carlson Trophic Index (1977).

The objective of this study is to use a satellite based approach for assessing the water quality concerning the trophic condition and sediment yield in Sazlıdere reservoir and to create thematic maps representing the distribution and concentration of quality indicators including secchi disk transparency, chlorophyll-a and suspended sediment. Furthermore, it will help to demonstrate the contribution of satellite data for a better understanding of the spatial and temporal characteristics of water quality within the reservoir through the observations from thematic maps of water quality indicators. Finally it intends to indicate that supplements of high resolution satellite observations to ground based water quality monitoring systems, such as synoptic overviews allows for enhanced visualization of water resources and their environments and thematic maps of water conditions assist in improving sampling strategies.

1.4 Benefits of the Research

This study will improve the understanding of the temporal and spatial dynamics of water quality indicators in water supply reservoirs and their controlling factors. It will thus contribute to the development of knowledge of reservoir water quality management. It will also exemplify the potential contribution of satellite data to the water quality assessment.

The understanding of temporal and spatial variations of quality variables regarding the mapping helps water management agencies to simulate change scenarios in reservoir water quality over time.

At a local scale, this study with satellite based assessment can provide valuable information for the better understanding of spatial and temporal characteristics of water quality in the Sazlıdere reservoir. It will also make it possible to generating a water quality data series for the reservoir to detect trends at various time scales. Furthermore the potential and contribution of remote sensing technology to water quality monitoring can be useful for water management authorities such as Istanbul General Directorate of Water and Wastewater (ISKI). ISKI manages the water quality of the reservoir with a ground based monitoring system. Also to protect the area adjacent to reservoirs and their watershed areas against illegal expansion, ISKI uses high resolution satellite data to monitor illegal housing and development. Although ISKI recently stopped obtaining this satellite data, this research can be helpful for its goals concerning water management applications In the future, real time satellite based monitoring systems for reservoirs under its authority can be implemented.

1.5 Thesis Structural Organization

This thesis is divided into five chapters. Chapter 2 presents background information about the development of remote sensing technology in water quality applications and image preprocessing procedures, which all improve the understanding of the materials and methodology used in this study. Chapter 3 presents the physical environment and land use of the Sazlıdere watershed which can contribute valuable primary knowledge to water quality assessment. Chapter 4 presents data collection and methods of study. Chapter 5 presents the results and limitations of this study and its conclusions.

CHAPTER 2

LITERATURE REVIEW

2.1 Introduction

This chapter aims to introduce the basic knowledge on which this research is based, and to provide background information to understand the methodological approach used in this thesis. In order to contribute to this purpose, the following issues will be mentioned: remote sensing technologies and water quality applications, the preprocessing of remote sensing data, the remote sensing method for water quality parameters, and the Trophic State Index.

2.2 Remote Sensing Technology and Water Quality Applications

Earth Resources Technology Satellite (ERTS-1), later renamed Landsat-1 is the first satellite of NASA used for environmental monitoring. It was launched in 1972 (Bukata, 2005). In last three decades, the Landsat 2-7 series have been providing multispectral data of the earth. These data have been employed for both terrestrial (Loveland *et al.* 2008, Goetz *et al.* 2004) and aquatic research (Iwashita *et al.* 2004; Pattiaratchi *et al.* 1994).

After the launch of ERTS-1, the number of airborne and space-borne sensor systems possessing advanced spectral and spatial resolution, and viewing capabilities have been increased (Bukata, 2005). Airborne instruments varying from imaging spectrometers to multispectral scanners instruments such as the compact airborne spectrographic imager (CASI), the airborne imaging spectrometer (AISA), the Airborne Visible/Infrared Imaging Spectrometer (AVIRIS), the Airborne Hyperspectral Mapper (HYMAP), the Moderate Resolution Imaging

Spectroradiometer (MODIS), and the Medium Resolution Imaging Spectrometer (MERIS) have been used for terrestrial and aquatic research interests. Regarding some airborne remote sensing applications, CASI imaging spectrometry data were applied to determine the presence and concentration of cyanobacteria in inland waters (Dekker *et al.* 1992). AVIRIS was used to investigate seasonal and interannual variations of plankton in Mono Lake, California (Melack and Gastil, 2001). Water quality parameters such as concentrations of dissolved organic matter (CDOM), chlorophyll-a and total suspended matter were mapped using a hyperspectral imaging scanner (Hakvoort *et al.* 2002). MERIS is the only multispectral sensor aboard a satellite that observes coastal and inland waters (Bukata, 2005).

Space-borne remote sensing with optical and thermal bands was used to evaluate water quality variability, including turbidity, chlorophyll-a, temperature and trophic level (e.g. Sass *et al.* 2007; Fuller *et al.* 2004; Islam *et al.* 2001; Giardino *et al.* 2001; Lathrop, 1992). Space-borne instruments such as the Landsat Thematic Mapper (since 1984) and SPOT-HRV have been used for inland waters (Dekker, 1993). Landsat TM has been employed for several water quality monitoring studies (Olmanson *et al.* 2008; Brivio *et al.* 2001; Dekker and Peters, 1993). As a result of Landsat satellite's synoptic coverage, 185km*167 km, water quality for large areas can be monitored in a single image.

Hyperspectral satellite remote sensing has also been used for water quality applications including monitoring nutrient content in an estuary (Gilbes-Santaella, 2008), mapping water quality concentrations of chlorophyll-a, colored dissolved organic matter, and suspended matter (Brando and Dekker, 2003). The use of

hyperspectral data has recently become widespread, while multispectral data (e.g. Landsat, SPOT, and AVHRR) have been used regularly since the 1970s (Shippert, 2004). Hyperspectral imagery having a very high spectral resolution and producing numerous narrow spectral bands provides the potential for more accurate and detailed information extraction of an object (Shippert, 2004). The launch of NASA's EO-1 Hyperion sensor brought about an era of space-based Hyperspectral remote sensing including the launches of ARIES, NEMO, and SIMSA. However, NEMO is the only Hyperspectral satellite sensor specifically designed for coastal and inland water imaging (Bukata, 2005).

With several recently launched satellite sensors including IKONOS, SPOT 5, and Quickbird 2, high spatial resolution satellite data have become widely available. These developments bring spatially extensive information that can be used for water quality assessments.

2.3 High Spatial Resolution Imagery and IKONOS

Advancements in remote sensing technology have provided sensors that have more spatial and spectral sensitivity. Those sensors' capabilities offer more detailed and more accurate information in earth observation images. Satellites with a higher spatial resolution and airborne systems capable of high spatial resolution imagery have been collecting data for remote sensing applications that is superior to their satellite borne predecessors for many years. The era of high resolution space-borne imagery began in 1999 with the launch of IKONOS-2 (Sawaya *et al.* 2003) providing 1 meter resolution imagery.

Several recent studies have used IKONOS for water quality assessment in small lakes (e.g., Sawaya *et al.* 2003; Folgo A Batista *et al.* 2003) and inlet waters (Ekercin, 2007; Sarıkaya, 2006). These studies stated that high resolution satellite data are efficient for the assessment and mapping of water quality characteristics. Providing greater spatial details, IKONOS gives more information about a surface and better visual interpretation of remotely sensed data than is offered with other types of satellite sensors (e.g., Landsat TM - 30 m pixels). This sort of spatial detail of images make it possible to see the effects of land use on lake water quality by overlaying thematic maps of water quality variables and IKONOS images (Sawaya *et al.* 2003). Another benefit of high spatial resolution data is that it makes classification categories highly customizable for continuous mapping variables such as water clarity (Sawaya *et al.* 2003).

The IKONOS scene size of 11 * 11km enables coverage of a smaller area in a single image than is provided by other satellite synoptic coverage (e.g., Landsat - 180*180 km). Because of this, it can be used effectively at water quality assessment of smaller lakes. For a regional water quality assessment, the cost of high-resolution imagery is getting expensive. To make it affordable, the imagery can be shared between departments and used for several applications. (Sawaya *et al.* 2003). The multispectral sensor of IKONOS allows measuring reflectance of water at a few wavelengths bands, while the bands allows for development of high resolution satellite applications based on past research as a result of compatibility with Landsat TM bands 1-4. This compatibility also makes it possible to use similar dates of Landsat data and field data alongside of the IKONOS image to generate a modeled relationship applied for water quality estimation (Sawaya *et al.* 2003).). Also, its

temporal resolution makes it possible to monitor the same area once every 1-3 days. This is a quicker revisit period than what has been offered by other satellites or data collection methods.

For effective use of satellite images in most of the remote sensing applications as well as with IKONOS data, before used in water quality assessment it is required that the data be preprocessed in some standardized approach.

2.4 Image Preprocessing

Image preprocessing is an initial processing of the raw image to correct any distortion arisen from sensor characteristics and environmental conditions that exists in the data (United Nations Environment Programme, 1995). The preprocessing includes a series of sequential operations such as geometric correction, calibration to radiance or at-satellite reflectance, atmospheric correction, and masking for unneeded features (Coppin and Bauer, 1996). Distortions resulted from sensor geometry and the effects of atmosphere on radiation process, producing during the image acquisition process, influence the quality of the remote sensing data. Therefore, elimination of all these effects from data before the data from the sensor are usable for analysis is important (UNEP, 1995) for getting more accurate information from satellite imagery. Moreover, transforming the data to ground coordinates and conversion to a meaningful physical unit allows for greater benefit with a quantitative purpose.

Geometric correction is usually performed by image vendors. For example, IKONOS provides a geometrically corrected image for its GEO products. Therefore, in image preprocessing it will be focused on removing atmosphere effects on the

image data and conversion of data from raw values to a physical unit. In the following sections, the procedure for radiometric normalization and atmospheric correction is described.

2.4.1 Radiometric Normalization

Radiometric normalization is a process that converts raw digital number (DN) values recorded by a space-borne or airborne sensor to physical units, such as radiance or Top-of-the-Atmosphere (TOA) reflectance. As each sensor sensitivity and scaling is different in recording the DN values, satellite data are not delivered in comparable and defined units (Geosystems, 2006). For instance, the same DN values taken by two images of different sensors may correspond to two different radiance values (Fleming, 2003). The raw DNs of satellite data need to be re-scaled into a defined spectral range. Each sensor provides its own calibration coefficients which consist of Offset (also called Bias) and Gain values. These coefficients are used to generate radiance values representing a defined physical unit. The sensors may have different mathematical equations to convert DN to radiance.

Space Imaging uses the following formula to calculate the IKONOS spectral radiance, $L\lambda$ (Geosystems, 2008):

$$L\lambda \text{ (mW cm}^{-2} \text{ sr}^{-1}\text{)} = \text{DN}/\text{CalCoef}\lambda \quad \text{(2. 1)}$$

Where: L is radiance at sensor aperture (mW/cm² *sr⁻¹).

DN = digital number

CalCoef_k = radiance calibration coefficient (mW/cm²*sr*DN)

The calibration coefficients for various bands of 8 and 11 bit products are provided by a Space Imaging in a document (Geosystems, 2008).

Converting DN values to TOA reflectance values is performed based on the simple reflectance relationship shown following equation. TOA reflectance is also known as planetary reflectance. IKONOS planetary reflectance values are calculated as follows (Fleming, 2003):

$$\rho_p = \pi * L_\lambda * d^2 / ESUN_\lambda * \cos(\theta_s) \quad (2.2)$$

ρ_p = planetary reflectance

L_λ = spectral radiance at sensor's aperture

ESUN = band dependent mean solar exo-atmospheric irradiance

θ_s = solar zenith angle

d = earth-sun distance, in astronomical units

The reflectance is determined by dividing by exoatmospheric irradiance. It is calculated without taking into account the atmospheric effects. In order to eliminate atmosphere interferences and calculate true ground reflectance, additional calculations obtained from atmospheric models are required.

Radiometric correction is important because it enables a physical base for quantitative relationship of satellite data and ground observations. Statistical models derived from this relationship are used to estimate surface characteristic variables. Furthermore the comparative analysis of optical properties of lake derived from different sensors make radiometric unit conversion as a necessary procedure (Brivio *et al.* 2001).

2.4.2 Atmospheric Correction

The observed radiance recorded by a remotely measured sensor contains both atmospheric and surface information (Warner *et al.* 2009). Irradiance (incoming solar

radiation at the surface) and radiance (solar radiation reflected from surface) are both affected by the atmosphere. Atmospheric effects occur by absorption and scattering. Absorption that reduces the radiation intensity (UNESCO, 1999) is caused mainly by atmospheric gases, such as water vapor, ozone, and oxygen plus aerosols. Water vapor is the most variable gas that significantly affects remotely sensed data (Liang, 2004). Absorption may affect radiance received by sensor reducing the DN that is assigned to the pixel (Gibson and Power, 2000).

Scattering that alters radiation direction results from interactions between electromagnetic radiation and both gas molecules (Rayleigh scattering) and aerosols (Mie scattering). It makes incident radiations diffuse in all direction. This scattering leads to the adjacency effect in which the radiance recorded for a certain pixel partially includes the scattered radiance from neighboring pixels (UNESCO, 1999). Thus it may reduce the image contrast and alter the spectral signature of ground objects as received by the sensor (Sahu, 2008) and scattering effect may increase the assigned DN (Gibson and Power, 2000).

Depending on the purpose the data will be used for, it may be necessary to do atmospheric correction on the data. Mather (2004) lists three scenarios in which atmospheric correction is necessary. The first case involves analyzing two bands of an image and using the ratio of the two. Shorter wavelengths show more scattering the longer wavelengths. The second case involves atmospheric interference. For example, when measuring sediment and biological materials close to the water's surface, the things being measured are less apparent in the sensors than what is found in the atmosphere. In this case, the atmospheric component must be removed according to the closest estimate. The third case involves ground measurements

taken at different times. Since atmospheric values may differ at different times, they must be adjusted for. They should be recorded and compared. After the atmospheric component is removed from a TOA signal measured by a sensor, only the surface related reflectance can be estimated.

To estimate the atmospheric effects from spectral data, atmosphere modeling approaches have been developed and implemented. For example, a physic-based approach derived from a radiative transfer model is designed to compute atmospheric effects of scattering and absorption. Radiative transfer models numerically simulate radiation transfer in the atmosphere for a given sensor geometry, surface elevation and atmospheric characteristics (Westmoreland, 2001) and calculate atmospheric path radiance arisen from both atmospheric emission and scattering, and atmospheric transmittances for scattering and water vapor allowing the surface radiance to be determined (Palluconi *et al.* 1999).

A radiative transfer model (RTM) can be used indirectly to generate atmospherically corrected data. This indirect use of RTM becomes more speedy than direct implementations of a RTM, while parameters are pre-computed and stored in lookup table for a range of viewing and solar geometries and atmospheric conditions. To estimate parameters specific to the image geometry and conditions, interpolation routines are used (Westmoreland, 2001). An example to this indirect method is Richter`s (1996) Atmospheric Correction (ATCOR) package (Westmoreland, 2001).

2.4.2.1 Atmospheric Correction in ATCOR

ATCOR is a software package for the atmospheric correction of multispectral and hyperspectral image data. ATCOR employs the algorithms based on MODTRAN

(Moderate Spectral Resolution Atmospheric Transmission Model) for the correction, and calculates ground reflectance values for each pixel of spectral bands. (Cincotta, 1997) As an ATCOR module, ATCOR2 is a spatially -adaptive fast atmospheric correction algorithm performing the correction over the flat terrain (Geosystems, 2008). The function (algorithm) for atmospheric correction is kept as look-up tables (LUTs) in the database. LUT is generated based on MODTRAN for a range of possible atmospheric cases. ATCOR LUT contains a significant range of each parameter defining atmospheric conditions. The values between are obtained by interpolation. These parameters and ATCOR's atmospheric correction components will now be described here primary based on documents of Geosystems, (2008).

Visibility ranging from 5 to 120 km is defined by the ground meteorological range. Also aerosol type is specified as urban, rural, maritime and desert. Both are used to model the aerosol effect. Input value for visibility can be obtained from metrological data. Selection of type of aerosol input depends on geographical location.

Solar zenith angle is ranged from 0° to 70° . ATCOR defines specific range values calculated for information on the solar irradiance above the atmosphere.

Ground elevation is ranged 0-2.5 km above sea level. Thus, contribution of Rayleigh scattering at each different elevation is taken account.

Water vapor ranges from 0.4 to 2.9 g/cm². Five standard atmosphere types (mid-latitude summer, US standard, tropical, fall and mid-latitude winter) are defined according to water vapor content range. There are several versions of each atmosphere in ATCOR 2, depending upon the sensor view geometry. For a sensor

such as IKONOS, which have omni tilt capability, the satellite elevation is used to determine the angle of the tilt. The tilt angles are specified as no tilt, 10, 20, or 30 degrees. The tilt direction is determined by the sun azimuth and satellite azimuth. ATCOR defines specific azimuth (30 deg= east, 60= south, 120= north, 150= west).

ATCOR2 is capable of particular functions such as spectra and atmospheric correction processing options which were performed for this study. Spectra module is produced based on the gray level values of an image. The module calculates and display reflectance spectrum taking account of the selected calibration file, visibility, and atmosphere model. With this derived spectra, the correctness of the selected values can be examined. The atmospheric correction processing option is performed with constant atmospheric conditions to derive the true spectral characteristic (reflectance) of surfaces.

The atmospheric correction procedure in ATCOR2 first converts DN to radiance at the sensor. ATCOR uses the radiance at sensor as a basis on the calculation of the atmospheric effects. The conversion of DN to radiance at the sensor is done by sensor calibration files provided with ATCOR2. The transformation is employed based on a simple linear relationship:

$$\text{Radiance (L)} = C_0 + C_1 * \text{DN} \quad (2.3)$$

ATCOR defines the offset as a C0 value and Gain as a C1 value. The calibration values C0, C1 calculated for all bands are stored in an ATCOR calibration file for each supported sensor. The calibration file provided for IKONOS does not work well in some cases. The verifying calibration file can be done using an automatic approach of the Spectra Module. A semi-automatic in-flight calibration file can be

generated by comparing a target within the image with reference spectra from ATCOR's database. This process generates the gain and bias values for each spectral band and automatically writes a new calibration file.

2.5 Development of Water Quality Parameters through the Remote Sensing Method

The basic principle of the remote sensing technique is that each type of surface objects or features depends on their physical and compositional attributes and reflects or emits a certain intensity of light at different wavelength ranges of the electromagnetic spectrum (Gupta, 2003). This radiant energy measured by remote sensing devices at various wavelength ranges provides information about each kind surface feature. Hence, using this radiant energy recorded by the remote sensing instruments makes it possible to discriminate between the different types of surface features and map their distribution on the ground (Gupta, 2003).

The use of remote sensing on water bodies depends on its ability to measure the variations of spectral response of the water (Ritchie *et al.* 2003). When water is pure or contains organic (e.g. chlorophyll-a) and inorganic constituents (e.g. suspended sediment), its absorption and scattering characteristics differentiate (Jensen, 2007). Those radiance components are measured by a sensor system at various wavelength ranges and then empirical or analytical relationships between the data and a water quality parameter are established through statistical analysis. The wavelengths are capable of capturing particular spectral properties of parameters. The substance, concentration and sensor characteristics of the target measurement must all be considered to determine the optimal wavelength to use to measure a water quality

parameter (Ritchie *et al.* 2003). When the quantity and proportion of each water constituents vary, it makes it difficult to yield accurate quantitative estimates of water content (Moses *et al.* 2009).

In freshwater systems, the most common pollutant in surface waters is suspended sediments. This is both in terms of weight and volume (Ritchie and Cooper, 2001). In both the visible and near infrared segments of the electromagnetic spectrum, radiance is increased by the presence of suspended sediments (Figure 2).

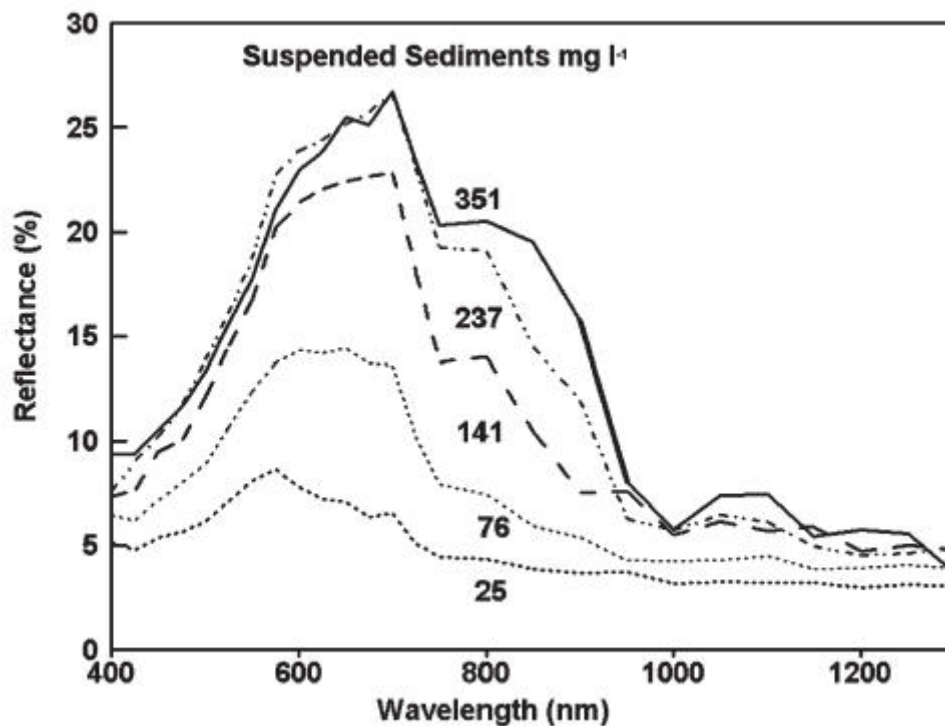


Figure 2: The relationship between reflectance and the electromagnetic spectrum for increased suspended sediment (Ritchie and Cooper, 2001).

The concentration of suspended sediment will significantly affect reflectance at most all wavelengths when suspended sediment levels are between 0 and 50 mg/l. When levels are above 200 mg/l, curvilinear relationships, viewing reflectance in longer wavelengths must be used (Ritchie and Cooper, 2001). Moreover the reflectance of

water is also changed by the presence of algal-chlorophyll concentration. Chlorophyll tends to reflect green, but absorb blue and red lights (Ritchie and Cooper, 2001); however in waters with high levels of suspended sediments, it is not possible to see chlorophyll levels using the broad wavelength spectral data currently available (Dekker and Peters, 1993; Ritchie and Cooper, 2001). This is due to the high spectral signal given off from suspended sediments. However, when more than one band is used, it may be possible to measure chlorophyll levels (Dekker *et al.* 1991). Chlorophyll *a* may be measured using bands between 400 and 900 nm, usually visible and NIR bands (Han and Rundquist 1997).

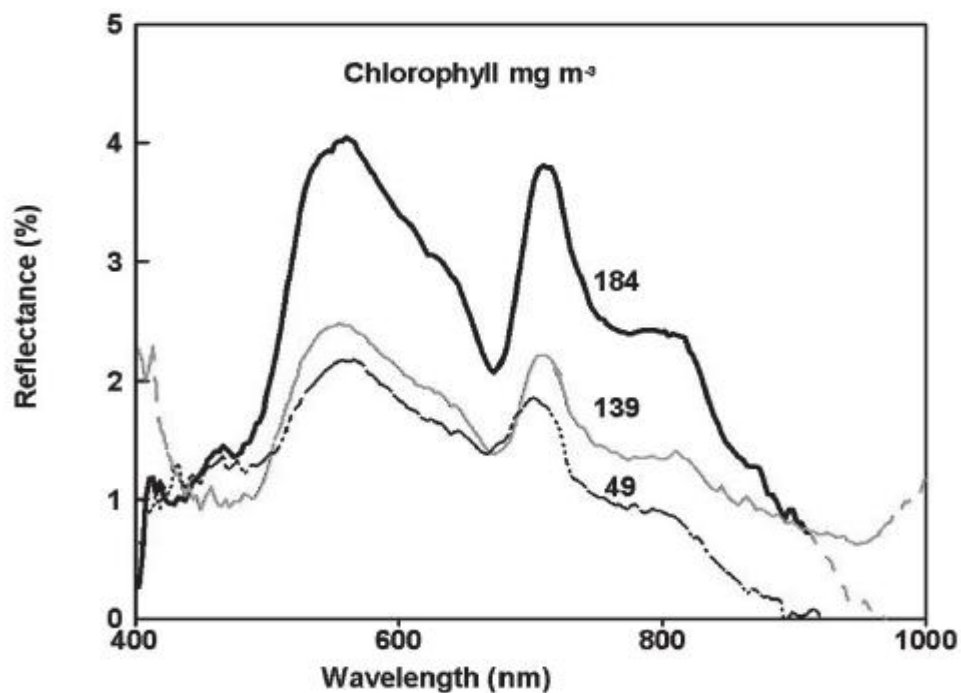


Figure 3: Reflectance across most wavelengths with increased chlorophyll concentration (Ritchie and Cooper, 2001).

In secchi disc, any visible substance, such as algae or suspended solids or dissolved substances will result in turbidity. There is a significantly higher visible

reflectance value in waters where turbidity is caused mostly by suspended sediments. The effect of chlorophyll on reflectance must also be remembered; it increases the green and decreases the blue and red wavelengths. Several studies have found blue and red band ratios to correlate well with SDT (Lillesand, 2001; Kloiber *et al.* 2002; Sawaya *et al.* 2003).

Ritchie and Cooper (2001) state that determination of nutrients in the water that do not change optical or thermal characteristics can must be determined by measuring other substances that may have been affected by the presence of those chemicals (for ex. an increase or decrease in chlorophylls). Phosphorus, for ex. cannot be measured directly by optical instruments, such as the Landsat Thematic Mapper, and there are some exceptions with no clear correlation between phosphorus and chlorophyll levels. Although broad band satellite platforms are not recommended to measure TP, several studies have correlated TP with satellite observations (Ke-Sheng *et al.* 1998; Yang *et al.* 1996; Sarikaya, 2006). , Also, the use of hyperspectral platforms to determine TP is becoming more accurate. For example, the Hyperion hyperspectral sensor has been used to show spectral profiles in the visible and near infrared bands in which nitrates and total phosphorus may possibly reflect (Gilbes-Santaella, 2008).

2.5.1 Empirical Approach

In aquatic remote sensing studies empirical method is generally used to relate spectral signatures from water recorded at the various bands to quality parameters (e.g. Sawaya *et al.* 2003; Dekker, 1993; Gitelson *et al.* 1993). This method uses statistical relationship derived between the measured spectral values and ground measurements of water parameters (Budhiman *et al.* 2004). Regression analysis is

utilized to establish the relation between those parameters, and produced a model using this statistical relationship of measured sample data, the model is applied to whole waterbody to predict water quality parameters.

By employing a spectral band as the independent variable and ground measurement of water quality parameters as dependent variables through regression analysis, a linear regression equation is developed. The linear regression equation attempts to explain the relationship between the dependent and independent (predictive) variables using a straight line (Sharma, 2009). When the linear regression includes more than one independent variable, it is termed as the multiple linear regressions (Rao *et al.* 2008). The general form of a linear regression is (Carr, 2002):

$$y^* = (c_0 + c_1x_1 + c_2x_2 + \dots + c_mx_m) \quad (2.4)$$

Where y is the dependent variable that will be predicted and estimated based on a linear combination of m independent variables, x

X values are independent variables (the combination of satellite bands or the bands ratio) that will predict Y .

The values, c , are coefficients that represent the effect of independent variables on the dependent variable Y .

In many previous researches, various band combinations and band ratios have studied to predict water quality parameters (e.g. Fuller *et al.* 2004; Giardino *et al.* 2001; Han and Rundquist 1997; Mittenzwey *et al.* 1992). As independent variables common optical bands used in aquatic remote sensing ranges from visible to near infrared regions. The best fit of band combinations are generally chosen based on

regression analysis, which takes independent variables of high R^2 for evaluation, and shows a correlation between the regression equation and existing data as values approach one. The chosen band combination is later used to construct model for predicting the water quality variable. There may or may not be a causal relationship between the parameters viewed, so results may be falsely interpreted (Yu, 2005; Budhiman *et al.* 2004). Before estimates based on the empirical models are accepted, they should be carefully evaluated. One problem connected to this approach is its heavy reliance on on-site data. With limited ground measurements or a lack thereof, this approach may not be accurate (Guan, 2009).

2.6 Assessing Water Quality Parameters

Water quality parameters provide useful information for the understanding of quality conditions and changes in the quality of a water body. They are used as criteria in assessing whether or not water is good for intended use. For identification of the water body with respect to parameters, water quality criteria are determined according to their designated use. Water quality criteria can be determined based on specific numeric values or a narrative form. The criteria index is developed based on key factors affecting water quality. For the assessment of trophic conditions, classification criteria can be developing dependent upon specific trophic quality indicators.

2.6.1 Carlson Trophic-State Index

The trophic state is a measure of a lake's biological productivity and is commonly used to determine water quality based on quantities of physical, chemical and biological determinants of the productivity. The Carlson's Trophic-State Index (TSI)

is a classification system broadly used in evaluating trophic conditions in lakes, which classifies a lake's productivity using key water quality indicators. These indicators are Secchi depth, Chl-a, and TP which are commonly used to determine the lake's water-quality characteristics (National Research Council, 1992). The Carlson's index ranges from 0 to 100 with each increase of 10 units. Each of these three index variables are linked based on the same index value. TSI values for each index variables are constructed based on following simplified forms of the equations (Gibson *et al.* 2000).

$$\text{TSI (Secchi disk)} = 60 - 14.41 \ln (\text{SD}); \quad (2.5)$$

$$\text{TSI (Total phosphorus)} = 14.42 \ln (\text{TP}) + 4.15; \quad (2.6)$$

$$\text{TSI (Chlorophyll-a)} = 9.81 \ln (\text{Chl-a}) + 30.6; \quad (2.7)$$

With chlorophyll-a and total phosphorus in $\mu\text{g/l}$ and Secchi disk in meters.

Ranges given for calculated of three index variables are determined for each trophic level, as presented in Table 1.

TABLE 1: TROPHIC STATE INDEX (Carlson and Simpson, 1996)

TSI	Chl (ug/L)	SDT(m)	TP (ug/L)	Attributes
<30	<0.95	>8	<6	Oligotrophic
30-40	0.95-2.6	8-4	6-12	
40-50	2.6-7.3	4-2	12-24	Mesotrophic
50-60	7.3-20	2-1	24-48	Eutrophic
60-70	20-56	0.5-1	48-96	
70-80	56-155	0.25-0.5	96-192	Hypereutrophic
>80	>155	<0.25	192-384	

Any three indicators may be used to determine the classification of a water body in terms of the TSI index. On the other hand, this may lead to multiple classifications for the same water.

The index shown in Table 1 ranges from 0 (ultra-oligotrophic) to 100 (hypereutrophic). The TSI index is divided into four parts which represent levels of biological productivity for the four trophic state categories: oligotrophic (low level), mesotrophic (moderate level), eutrophic (high level), and hypereutrophic (excessive level) biological productivity.

Oligotrophic waterbodies have a very low level of nutrients, little algae growth and a clear appearance (Dodds, 2002). Mesotrophic waterbodies generally have moderate nutrients and algae growth, and their appearances are moderately clear. Eutrophic waterbodies have low oxygen levels, high nutrient concentration and algae/plant growth, indicated by a green, cloudy and murky appearance (Dodds, 2002). Hypereutrophic waterbodies have excessive level nutrients and an abundance of algae (Carlson and Simpson, 1996).

CHAPTER 3

THE PHYSICAL ENVIRONMENT AND LAND USE OF THE SAZLIDERE WATERSHED

3.1 Introduction

Chemical contaminants and sediment from land, largely responsible for water quality problems, are carried in water and discharged into a nearby stream or reservoir (De la Cretaz and Barten, 2007). Land disturbing activities, the removal of natural vegetation and effects of human land use can cause changes in land structure and function. Loads of pollutant and sediment introduced by overland flow from agricultural and construction areas, storm water runoff from urban areas, and municipal and industrial wastewater may increase the rate of nutrient and sediment concentrations of a reservoir. The amount of pollutants and sediment loading into a stream are influenced by the combination of a region's climatic regime and watershed characteristics, such as topography, soil characteristics, and geology (De la Cretaz and Barten, 2007). Soil characteristics, geology, topography and the climate of the distressed region affected by human activities can contribute to water quality problems by increasing the level of pollution.

To be familiar with the physical environment and land use in a watershed can be useful for understanding the processes that affect water quality. These kinds of information provide a base for interpreting the distribution and concentration of water pollution in a reservoir. With the help of this background knowledge and the mapping of water quality variables estimated using satellite imagery over the whole

reservoir surface, the spatial and temporal changes of pollution, and therefore the water quality of a reservoir can be evaluated.

In this chapter the climate, land use and physical environment of the Sazlıdere watershed are described, explaining their possible effects on pollutants and sediment discharges to the reservoir.

3.2 Effects of Climate on Water quality

The climate factor including precipitation, temperature and wind of seasonal variables can affect water quality in many ways. The most important contributor to runoff, erosion, and sediment inputs is rainfall (Soil and Water Conservation Committee, 2009). Heavy rainfall increases the water's ability to remove soil and transport its particles as well as its capacity for carrying surface containments (SWCC, 2009). Thus, sediment and chemical inputs to nearby water resources are increased by the runoff associated with rainfall.

During the summer, due to dry surface conditions, soil particles from dried bare fields can be moved by strong winds and transported to the water surface. Strong winds can also generate waves, which can significantly influence turbidity in a shallow water body causing sediment resuspension. Resuspension can also increase the flux of nutrients found in the sediments at the water body. Increases in temperature can evaporate large amounts of water and reduce dissolved oxygen levels in water (Murphy, 2005). Also due to high temperature and lack of rain, the water level in a lake can decrease; chemical reactions in water can increase, and simultaneously can affect biological activity and growth. These conditions may result in algae blooms that increase turbidity.

When extreme precipitation events happen, runoff from these events result in flooding and can cause an increase in pollutants and sediment from urban, industrial and agricultural areas.

3.2.1 Temperature and Precipitation Characteristics in the Watershed

The climate regime of the reservoir's basin is typically characterized as hot and dry in the summer, with winters that are rainy and moderately cold. The drainage basin can be divided into three regions (southern, western and northeastern) based on distribution of the mean annual precipitation categories in the Istanbul (Erinc, 1980). For the assessment of the climate regime of the study area, three meteorological stations located close to the regions were used. Between 1975 and 2008, the average of total annual precipitation recorded at Çatalca, Florya and Bahçeköy Meteorological Stations, is about 775.4 mm.

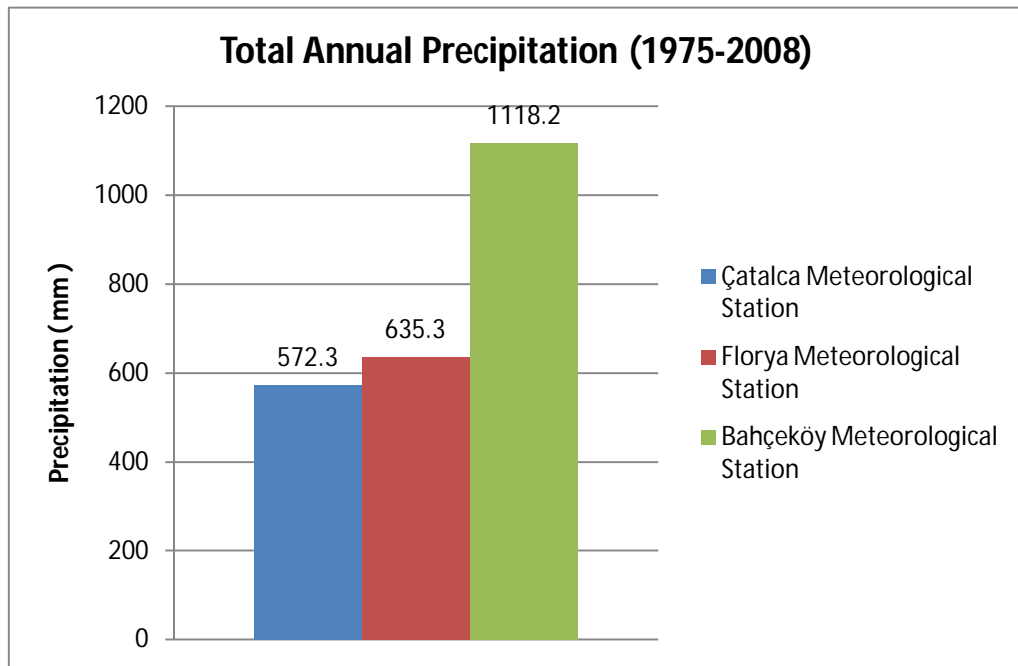


Figure 4: Total annual precipitation in the Çatalca, Florya and Bahçeköy Meteorological Stations between 1975 and 2008.

According to the total annual precipitation data of these stations locations for the same period, the precipitation in the western portion of the watershed declines, as you move southward the precipitation increases. In the northeastern area, have the highest amount of precipitation (shown in Figure 4). During this period, the mean temperature recorded in three stations for winter is about 5.58° C; in summer it is about 22.6° C.

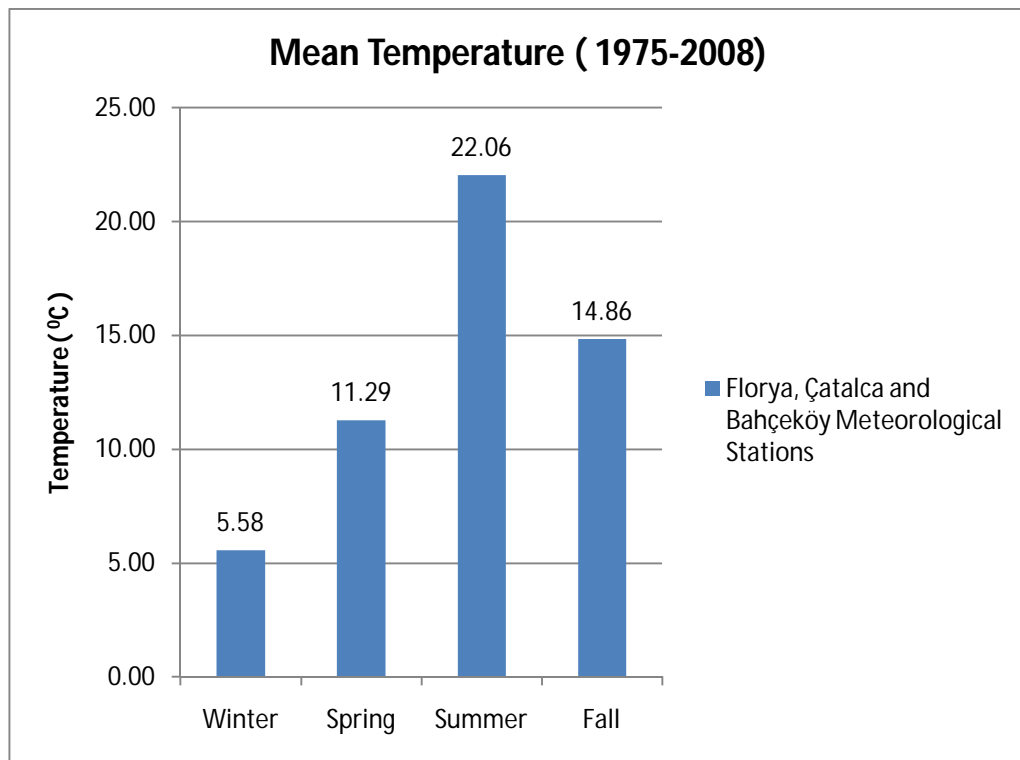


Figure 5: Average Temperature of the Çatalca, Florya and Bahçeköy Meteorological Stations between 1975 and 2008

Dry conditions in 2007 caused extreme drought. A total of 165.7 mm of precipitation fell during the 9 month period which is below the average (January-September) compared to a long term average of 383.6 mm (Figure 6).

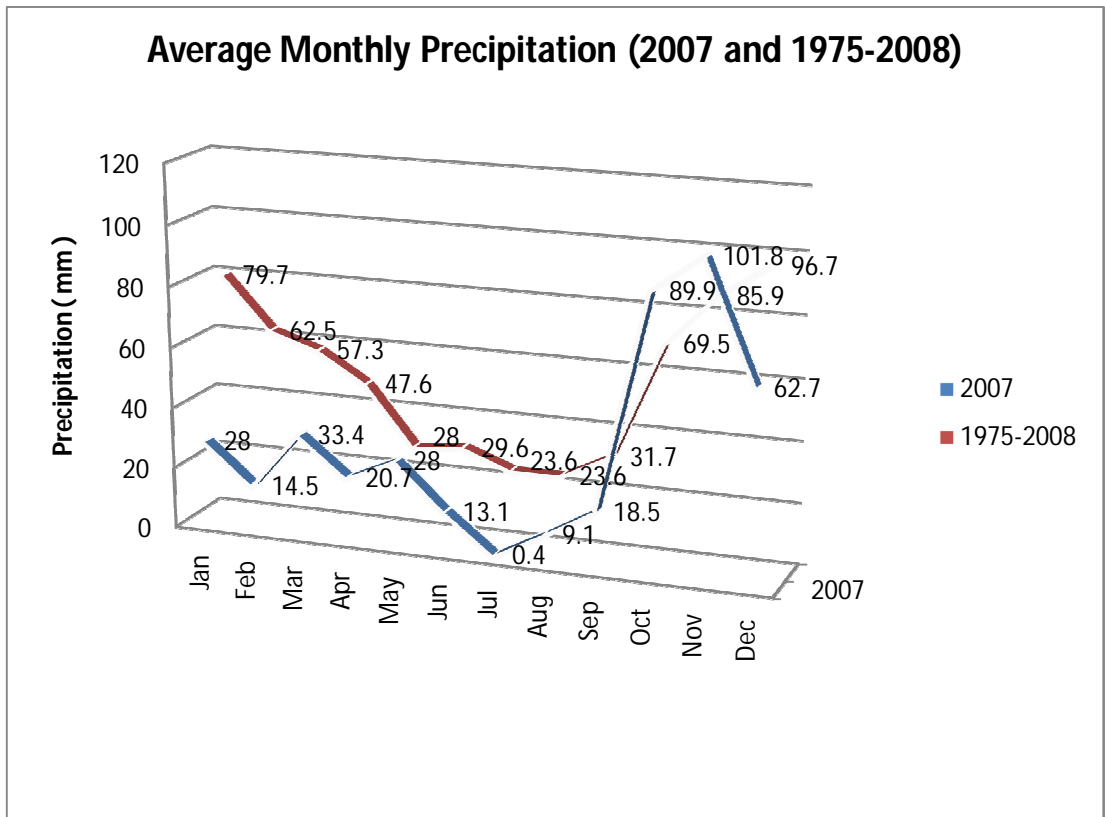


Figure 6: Comparison of the average monthly precipitation between 2007 and 1975- 2008 (Florya Meteorological Station).

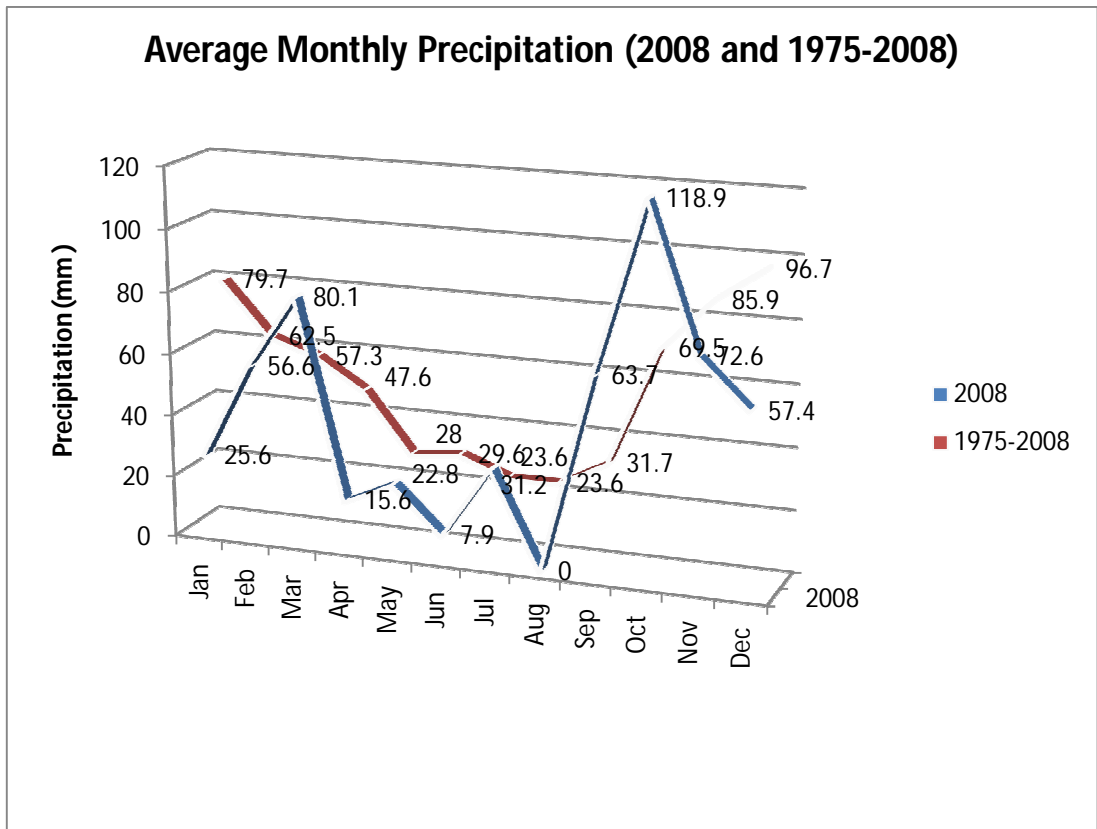


Figure 7: Comparison of the average monthly precipitation between 2007 and 1975-2008 (Florya Meteorological Station)

The total annual precipitation in 2007 and 2008 is below the long-term (1975-2008) average (Figures 6-7).

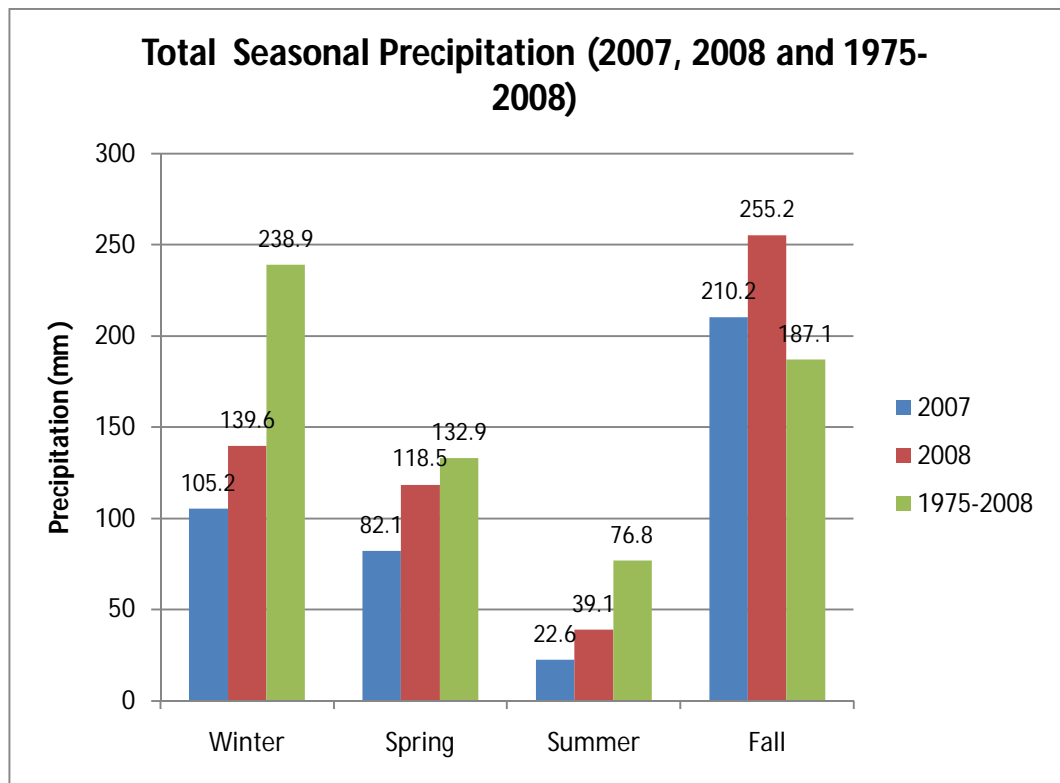


Figure 8: The total seasonal precipitation in 2007, 2008 and 1975-2008 (Florya Meteorological Station).

Precipitation in winter, spring and summer during 2007 was below the long term average, except for the spring. For the fall, precipitation increased compared to the long term average. Throughout 2008, the rate of precipitation was still below the long term average for the same period, as was the rate in 2007. In comparing these two years of precipitation, 2007 was lower than 2008. The temperature in 2007 and 2008 is slightly above the long-term average. The temperature in 2007 was higher than that of 2008.

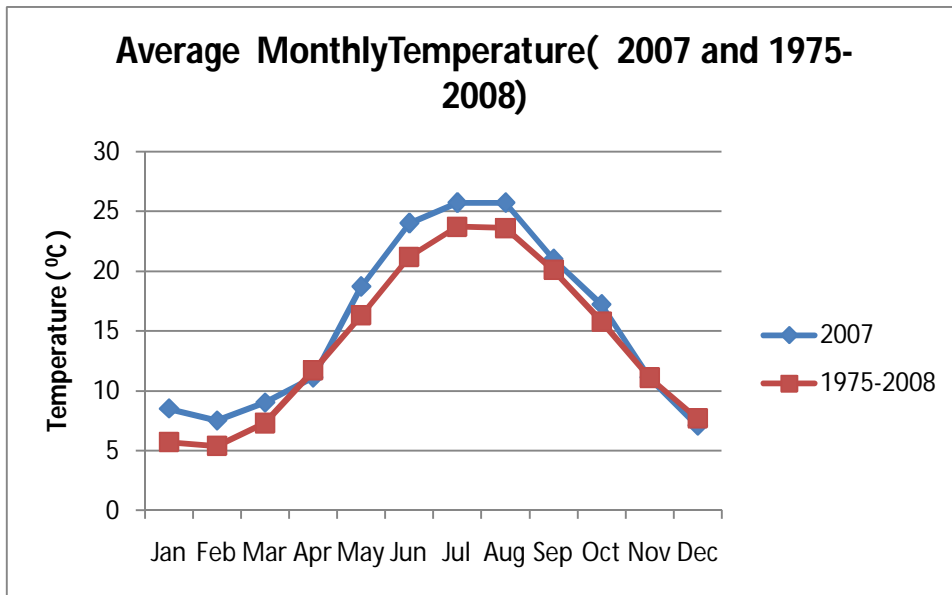


Figure 9: Comparison of the average monthly temperature between 2007 and 1975- 2008 (Florya Meteorological Station)

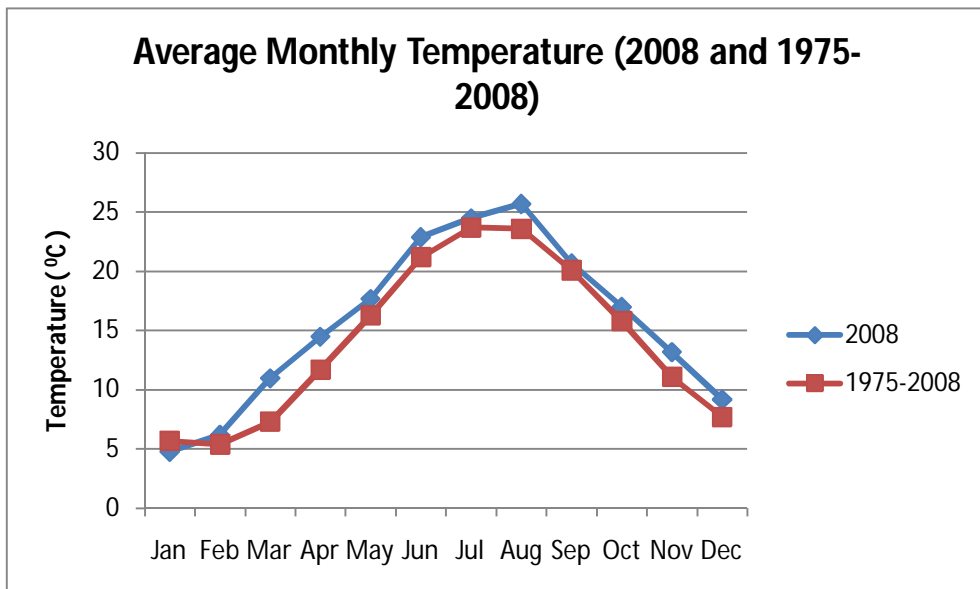


Figure 10: Comparison of the average monthly temperature between 2007 and 1975- 2008 (Florya Meteorological Station).

3.2.2 Water Level Changes in the Reservoir

Changes in precipitation and runoff to the reservoir affect variations in water levels. The lowest levels occur during periods of scarce precipitation and high temperatures that increase evaporation. During periods of high lake levels, storms can increase sediment and nutrients loading into the reservoir through runoff. Although there is no potential for external loading of sediments and nutrients into the reservoir during periods of low water levels, resuspension from reservoir bottom sediment can occur so that suspended sediment and nutrient concentration in the reservoir water can increase. Reflecting the dry conditions in 2007 and 2008, low water levels occurred (Figure 12). The amount of runoff discharged into the water supply reservoirs in Istanbul showed the same trends as the precipitation rate of the Sazlıdere reservoir in 2007 and 2008 (Figure 11).

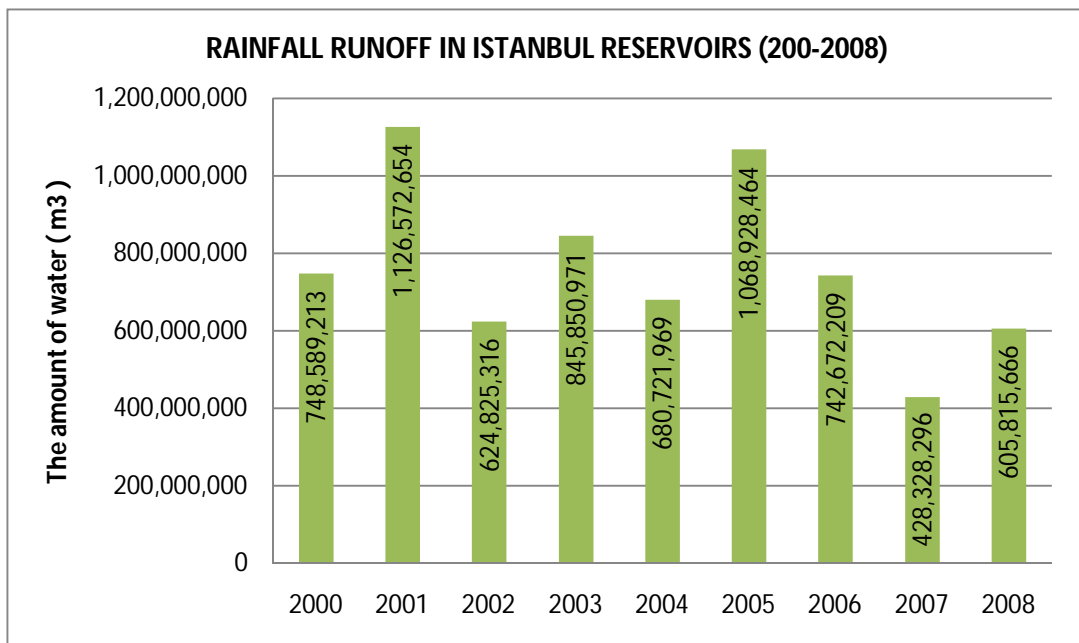


Figure 11: The amount of runoff discharged into the water supply reservoirs in Istanbul from 2001 to 2008 (www.iski.gov.tr accessed May 30, 2010).

Although there had been higher precipitation and runoff in 2008 compared to 2007, 2007 was characterized by higher water levels throughout the reservoirs.

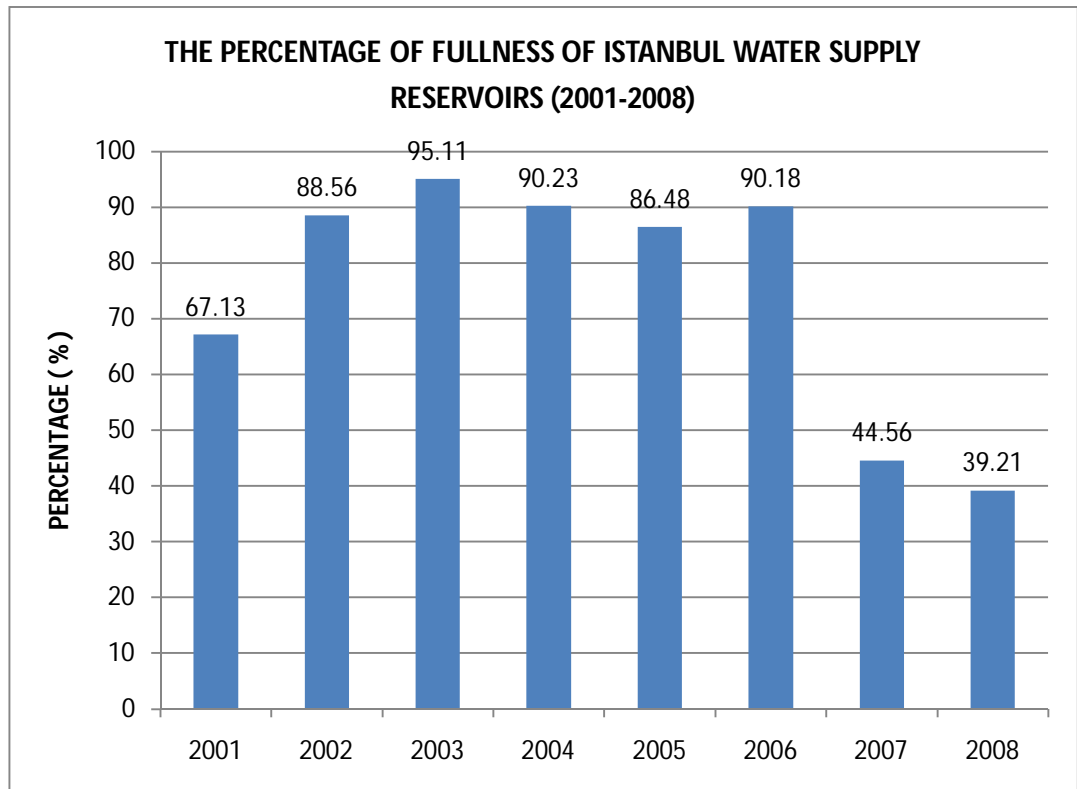


Figure 12: The percent filled to capacity of Istanbul water supply dams on May 30 from 2001 to 2008. (www.iski.gov.tr accessed May 30, 2010).

Since, high levels in precipitation and runoff occurred during former years, the reservoir's levels gradually lowered in 2007(Figures 11-12).

3.2.3 The characteristics of winds in the watershed

TABLE 2: THE PREVAILING WIND DIRECTION (1975-2008)

PREVAILING WIND DIRECTION (1975-2008)			
Stations:	Florya	Çatalca	Bahçeköy
Jan	NNE		
Feb	NNE		
Mar	NNE	N	
Apr	NNE		
May	NNE		
Jun	NNE		
Jul	NNE	N	NE
Aug	NNE		
Sep	NNE		
Oct	NNE		
Nov	NNE		
Dec	NNE	N	
ANNUAL	NNE	N	NE

TABLE 3: THE PREVAILING WIND DIRECTION (2007 - 2008)

MAXIMUM WIND SPEED (m/sec) AND ITS DIRECTION				
STATION:	ÇATALCA	FLORYA	ÇATALCA	FLORYA
	2007	2007	2008	2008
JAN	36.0/SSW	16.7/SW	30.1/NNE	18.9/NNE
FEB	31.0/N	13.9/NE	27.4/NE	20.7/NE
MAR		15.8/NE		15.7/WSW
APR	20.3/N	15.0/NE		13.7/SSE
MAY	19.6/NNE	12.6/NE		17.7/NNE
JUN	20.7/NNE		18.3/WNW	12.7/ENE
JUL	19.1/NNE	14.4/NE	23.8/N	13.8/N
AUG	26.3/NNE	16.1/N	22.7/ENE	15.4/N
SEP	23.8/N	16.4/NE	27.3/NE	18.3/NW
OCT	20.3/N	13.0/NE		15.4/WSW
NOV	27.2/NE	16.1/SSW	33.5/SSW	19.4/WSW
DEC	23.6/N 23.6/NE	14.9/NE	24.5/NE 24.5/NNE	15.2/NE

TABLE 4: MAXIMUM WIND SPEED AND ITS DIRECTION (2007 - 2008)

MAXIMUM WIND SPEED (m/sec) AND ITS DIRECTION				
STATION:	ÇATALCA	FLORYA	ÇATALCA	FLORYA
Day	(May, 2007)	(May, 2007)	(May, 2008)	(May, 2008)
1	11.1 / NNE	7.6 / NNE		4.1 / SW
2	17.2 / NNE	8.8 / NNE		6.8 / NW
3	7.0 / ENE	5.0 / NE		7.3 / NW
4	10.0 / NE	8.0 / NE		6.6 / NNE
5	6.5 / SSW	3.9 / W		7.9 / N
6	13.8 / ENE	10.3 / N		9.0 / NNE
7	13.7 / WNW	9.8 / WNW		8.8 / ENE
8	13.0 / SW	7.6 / N		11.1 / NNE
9	8.6 / WNW	4.7 / WSW		6.4 / N
10	13.6 / NNE	10.4 / N		5.3 / ENE
11	10.2 / S	8.8 / N	9.9 / NE	7.9 / N
12	8.5 / NNE	6.2 / N	9.3 / NE	7.8 / ENE
13	14.0 / N	8.7 / NNE	7.4 / NNE	4.6 / SW
14	14.1 / NE	12.6 / NE	10.8 / ENE	7.8 / NNE
15	16.0 / NNE	8.6 / N	13.4 / NNE	10.2 / N
16	11.0 / NNE	5.1 / NNW		6.0 / ENE
17	11.4 / SW	5.9 / ENE		4.5 / SW
18	17.8 / SW	8.2 / E		4.8 / ENE
19	18.5 / NE	9.4 / NNE		4.1 / NNE
20	19.6 / NNE	10.0 / N		3.6 / E
21	13.6 / SSW	6.2 / SW		8.3 / E
22	9.6 / NNE	8.7 / NNE		11.1 / WSW
23	8.5 / NNW	5.5 / SW		5.2 / W
24	8.0 / N	5.7 / SW		6.4 / W
25	7.2 / NE	5.6 / NE		5.9 / WSW
26	13.0 / WNW	7.1 / NNE		8.4 / NE
27	12.9 / WSW	5.7 / SW		5.5 / ESE
28	13.3 / SSW	7.3 / SSW		5.8 / W
29	16.0 / SSW	6.7 / SW		17.7 / NNE
30	9.6 / SSW	6.1 / W		9.4 / NE
31	9.2 / W	7.4 / SW		6.2 / ENE

The prevailing wind data of catchment area recorded in Çatalca, Florya and Bahçeköy Meteorological Stations on an annual basis from 1975 to 2008 (Table 2) indicated prevailing wind flow in N, NNE, and NE directions. NNE is the prevailing wind direction from January to December recorded at the station of Florya. For the same period north winds dominated in the Çatalca Station for March, July and November. For the Bahçeköy Station NE prevails in July.

As for May 2007 (Table 3), a maximum wind speed of 19.6 m/sec and a direction of NNE were recorded at the Catalca Station. For the same period recorded in Florya Station, the maximum wind speed and its direction is 12.6 m/sec NE. As for May 2008 maximum wind speed is 17.7 m/sec and its direction is NNE recorded in Florya Station. According to the wind speed data during May 2007 (Table 4) which evaluated based on Beaufort-scale (Iceland Meteorological Office), five days had maximum wind speed ranges greater than 13.8 m/sec (near gale) with a flow mostly from N to ENE directions. A four day range greater than 17.2 m/sec (gale) with NNE, NE and SW directions was recorded in the Catalca Station; at the Florya station only one day is greater than 10.8 m/s with NE direction, which is a strong breeze. During May 2008 (Table 4), at the Catalca station only two days range greater than 10.8 m/s, with ENE and NNE direction which is strong breeze. At the Florya station only two days had a strong breeze, with NNE and WSW directions; and one day had gale with a NNE direction. Northeasterly winds are the norm. The waves caused by these winds are responsible for disturbing sediment. Overall winds ranging from north to northeast are dominant at the both stations. The winds can affect resuspension caused by wind generated waves at the shallow part of the reservoir. This can affect turbidity and the nutrient flux between sediment.

3.3 Land Use and Water quality

In urbanizing areas, most of the watersheds include a mix of urban, suburban, agricultural, and forested areas as well as a network of roads. Each land use in the watershed affects water quality in varying proportions. Urban influences and land use affect the aquatic environment in many ways. When its natural vegetation is cleared off the land and disturbed for construction at residential areas, for roads, commercial development, and industrial uses, it can be exposed to intensive erosion. Sediment resulting from erosion at construction sites is carried through runoff to close streams and reservoirs. The amount of sediment loading from a construction site depends on the area of the disturbed soil (De la Cretaz and Barten, 2007). Another effect of urban areas on water quality occurs after the land is covered with impervious materials such as buildings, paved roads and parking lots (Barnes et al, 2001). In these paved or impervious areas, water is not infiltrated from the surface. This causes all precipitation to be released as runoff. The acceleration of runoff caused by intensive storms may lead to flooding. All pollutants from urban areas such as industrial sites, and roadways are carried with runoff to streams, then to reservoirs. When combined sewer systems which collect both storm water runoff and sanitary sewage in the same pipe exceed their capacity during intensive rainfall, they overflow and discharge untreated wastewater directly into streams (EPA, 1999). During the event of heavy rain, this sort of sewer system can contribute high loads of solids, nutrients and heavy metals into streams. The effect of agricultural land use on water quality occurs in various ways. The tillage or ploughing of agricultural land increases soil disturbance. Soil becomes more prone to erosion. Runoff carries nitrogen and phosphorus, while pesticides and other chemicals are stored in the soil

(Ongley, 1996). Pollutants either bond to soil particles or are transported in soluble form in this surface water movement to streams, then to nearby water bodies. Transportation of pollutants usually happens during heavy rainfall events. Nitrogen and phosphorus are found in excess due to the overuse of fertilizers, both manure based and chemical based, which contain these two chemicals. (De la Cretaz and Barten, 2007). Moreover a site can suffer from continuous erosion by rain water in cases where land is stripped of its natural vegetation for farming purposes (Zink, 1939).

Forest areas in a watershed can affect water quality through runoff from disturbed forestland. When vegetation is removed, soil and hill slope surfaces are disturbed by any activity in a forested area; this may increase the potential for soil erosion, and thus sediment delivery to the streams. Unpaved and unplanned forest roads can produce a large quantity of sediment. When soil is compacted on these road surfaces, infiltration decreases and sediments and nutrients through runoff can be transported to streams.

3.3.1 Land Uses in the Watershed

The land use pattern in the Sazlıdere catchment area is characterized by mixed land use: urban, suburban, agricultural, and forest areas. Agriculture is the most dominant land use activity.

The west side of the watershed is mostly agricultural, while the east side is roughly half agricultural, with the other half consisting of forests and urbanized areas. There are pockets of developed areas in the agricultural area which surrounds the reservoir.

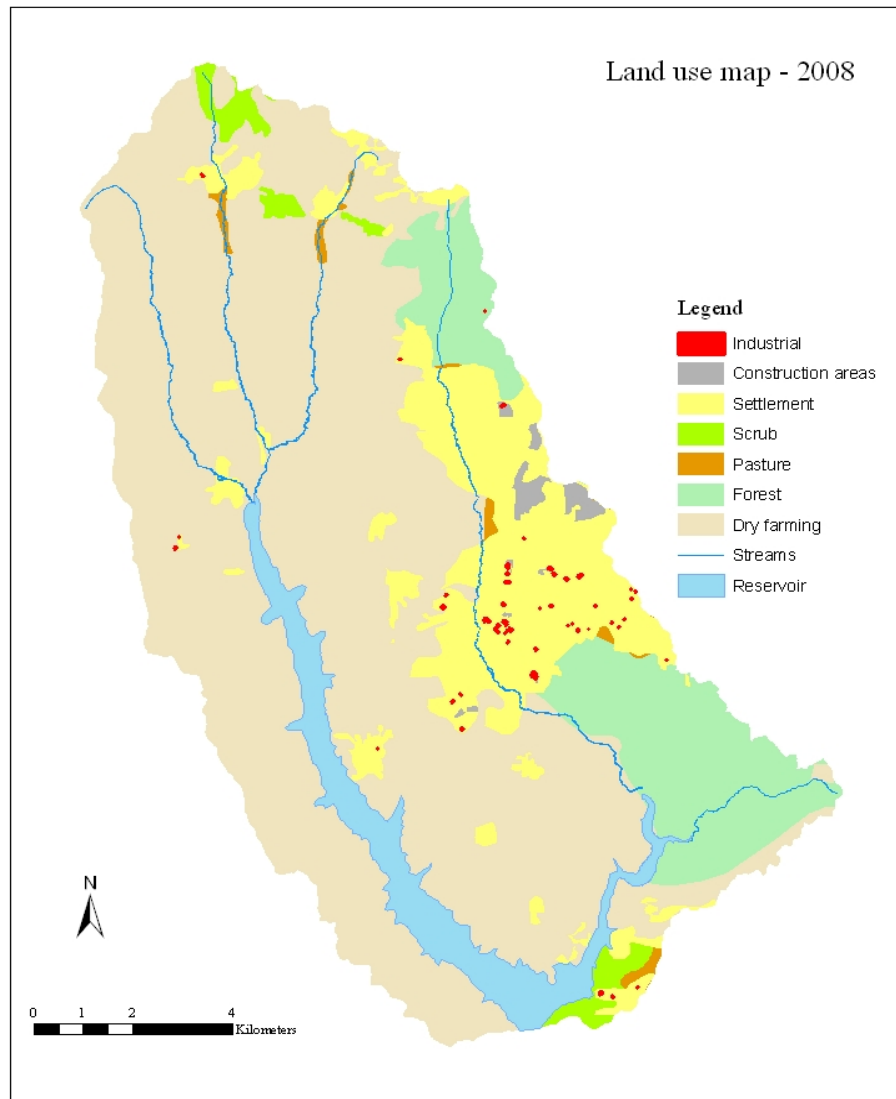


Figure 13: Land use map of the watershed

The agricultural area is mostly used for dry farming. With dry farming practices soil can be disturbed and become more prone to erosion. In the dry-farming region where the surface soil is left bare through tillage for preparation of seedbeds, especially on slopes, the soil results in intensive water erosion after heavy rainfall. Also the use of fertilizer for increasing crop production can contribute to nutrient loading into the reservoir.

The east side of the watershed is highly urbanized (Figure 13). Towns and small settlements in the catchment area have also separated around streams and the reservoir. Also new developing areas occur in the urban land, and sediment from these construction areas can contribute to pollutant-loading of runoff. Industrial land use mostly surrounds the stream, which might lead a greater potential for water quality impact. Furthermore the whole of the urbanized area in the watershed is managed by a combined sewer system which drains area of approximately 28078313.125 m² with 145866.35 meter of lines. Turkkose stream runs through the totally urbanized area before reaching a forested area, and later the reservoir. It collects rainwater runoff, domestic sewage, and industrial wastewater during heavy rainfall events when municipal combined sewers systems exceed their capacity. Sediment and nutrient pollutants from storm water runoff and sanitary sewage are discharged into the stream.

A small portion of the watershed is covered by forest found in the northeast and southeastern parts of the reservoir. The forest area in the southeastern of the reservoir has some steep slopes. With the characteristics of these slopes the area can be susceptible to erosion. Also the road system in the forest areas is mostly made up of forest roads that are found in flat areas which are surrounded by hills and reach into the streams. They can channel overland flow to streams. This may increase soil erosion and sediment delivery. The area is intensively eroded according to water erosion data (Figure 17). This leads to an increase in sediment and nutrient loading through runoff from hillsides to the reservoir.

3.4 Topography

Topography affects water quality through affecting runoff. Erosion from hill slopes can detach and transport soil particles due to rainfall and runoff effects. Shape and slope characteristics affect the amount and duration of runoff. The greater the slope length and steepness, the greater the potential for runoff, erosion and sediment delivery (SWCC, 2009). Soil on the hill slopes disturbed by agricultural activities such as tillage can cause greater quantity of sediment delivery.

The watershed is roughly half covered with flat to gently sloping hills and mostly used for agriculture. The areas of the three tributaries in the north, also used for agriculture, are semi-flat, with moderately sloping hills around the tributaries. The fourth tributary on the east side is also low and flat except for the area closer to the reservoir. This is a forested area where the land falls steeply down towards the water. The area southwest of the reservoir has slightly and moderately sloping hills.

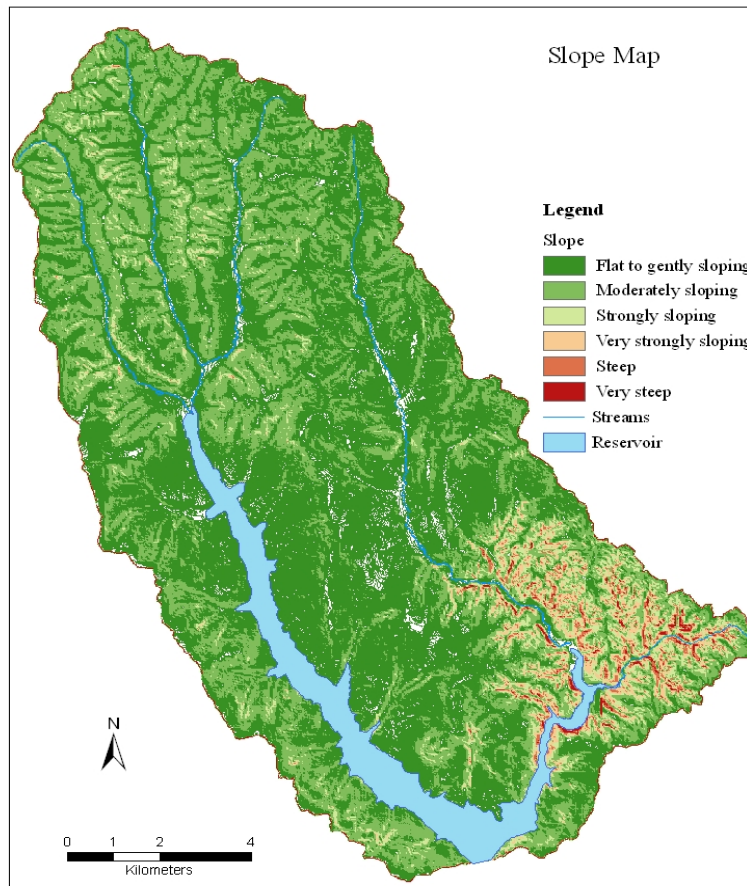


Figure 14: The slope map of the watershed.

Slopes are divided into six categories: $< 7^\circ$ Flat to gently sloping; 7° - 15° Moderately sloping; 15° - 20° Strongly sloping; 20° - 25° Very strongly sloping; 25° - 30° Steep; $>30^\circ$ Very steep (Sheng, 1990).

There is a relatively high elevation increase between the reservoir and the surrounding hills. Within the watershed area, altitude ranges from 5m to 235m. The average elevation is 120 m. As a result of the topography in the reservoir watershed, the erosion risk can be great during periods with heavy rainfall. Areas with steep or moderate slopes that are close to the flow of pathways can deliver soil particles to the streams.

3.5 Geology

Geology plays an important role in the surface formation within a site. Processes like landslides and erosion, the type of rock and its permeability are important factors. For instance, certain types of rock are more susceptible to chemical reactions, in other words, they are easily dissolved and breakdown in water so they are more prone to erosion. Also the chemicals weathered from rock in the catchment are carried by runoff into water bodies. This can affect the quality of water. The permeability of rocks is essential for the movement of water through the ground. Permeability affects how fast water moves through. In simple terms when water moves rapidly into the ground, the water penetration rate is increased and less runoff occurs, decreasing the amount of surface erosion.

The geological map indicates that the Sazlıdere catchment area (Figure 15) lies in four main geological formations: major part of the catchment area is covered by volcanic and sedimentary rocks of the upper Eocene-lower Oligocene. Carbonate and clastic rocks are exposed at the forest areas of the catchment. These are characterized as the Sazlıdere and Thrace formations and were determined as impermeable areas (Arparslan et al, 2006).

Neritic limestone of middle-upper Eocene rocks is in scattered areas in the central and southeastern area of the catchment. Because limestone tends to be soluble by water, the area might be partly damaged by erosion. Undifferentiated quaternary rocks overlie the reservoir bed. Undifferentiated Continental rocks of Pliocene are in small areas in northeastern of the catchment area.

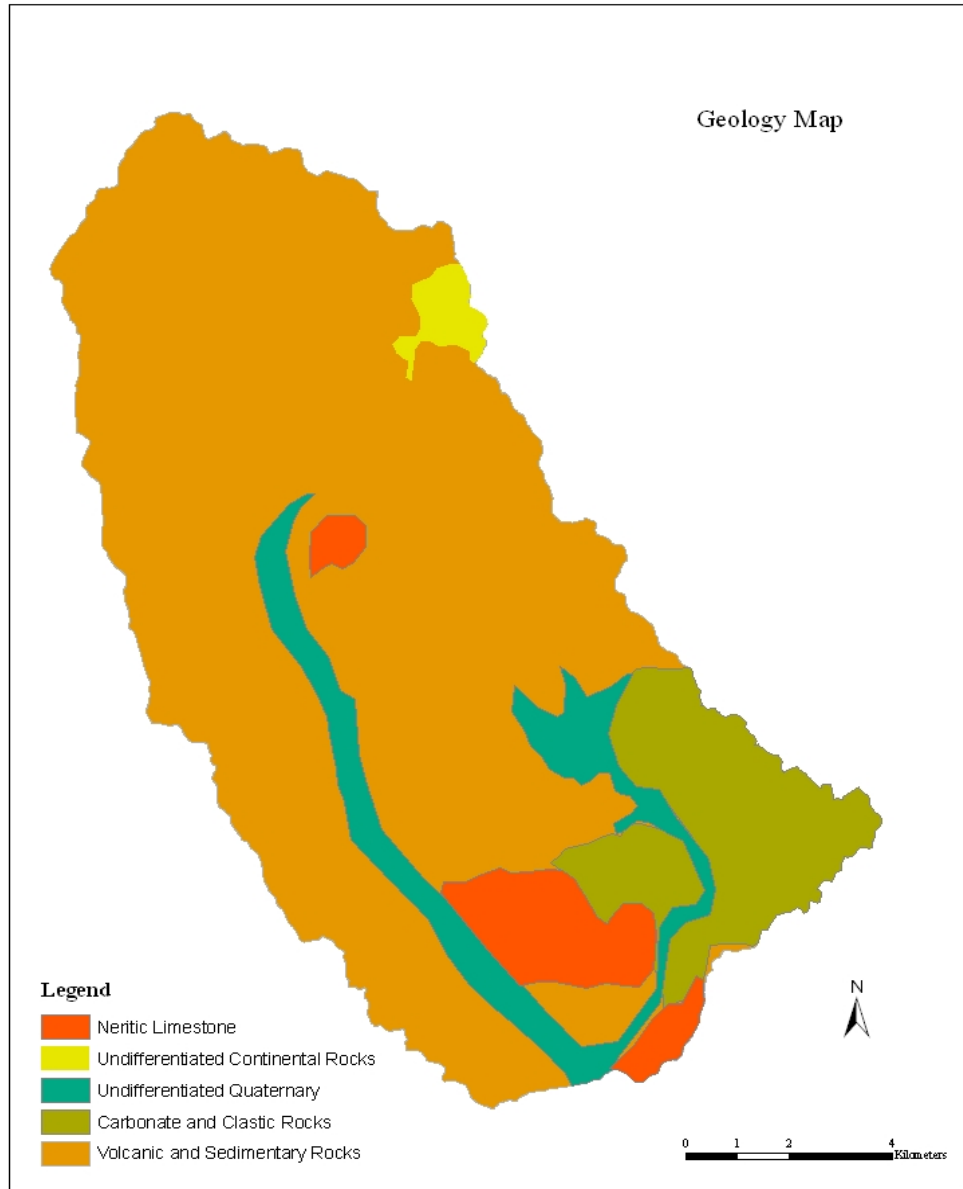


Figure 15: Geological map of the Sazlıdere catchment area (produced from the original Geological Map of Turkey, General Directorate of Mineral Research and Exploration, 2002).

3.6 Soil

Soil characteristics (e.g. structure, texture) and conditions (soil cover) are primary determinants in resistance to erosion (Sullivan, 2004). The capacity of soil to absorb water and the degree of movement of water through the soil profile and vegetative cover are important factor in lowering erosion risks at a site (Wells, 1988). When soils are less capable of being infiltrated by water, more tend to accelerate runoff. Soil in areas with steep slopes and lacking vegetation cover tend to have high erosion risks and to contribute sources of sediment and adsorbed pollutants to nearby water bodies.

The primary soil type in the catchment area is rendzinas (Figure 16). These soils were formed mostly from carbonate rocks. The common characteristics of rendzina are that they include high calcium carbonate contents and limited depths (Singer, 2007). The areas, in which rendzina are common are characterized by sloping topography (figure 14). The shallowness, underlined by the impervious rock surface and stony structure of the soil tends to limit water movement.

Soils in the southeast and northeastern area of the catchment are lime-free brown forest soils underlying forest areas (Figure 16). These kind soils are deep and include high organic layers (Lal, 2006). When these are covered by forest vegetation the high humus content prevents surface runoff, thus makes it resistant to erosion.

The area underlined by the one stream and reservoir body in the catchment is covered by alluvium (Figure 16). The area covered by these recently deposited materials can be easily eroded thorough heavy rainfall. The other soil which occurs in the northern stream and partial reservoir bed of the catchment is vertisol.

These include high clay with swelling content (Blokhuis, 1993). Under intensive rainfall, climatic conditions are susceptible to severe soil erosion (Virmani, 1988). Under certain climatic conditions, these soils within streams and the reservoir bed tend to be susceptible to erosion in the floodplains.

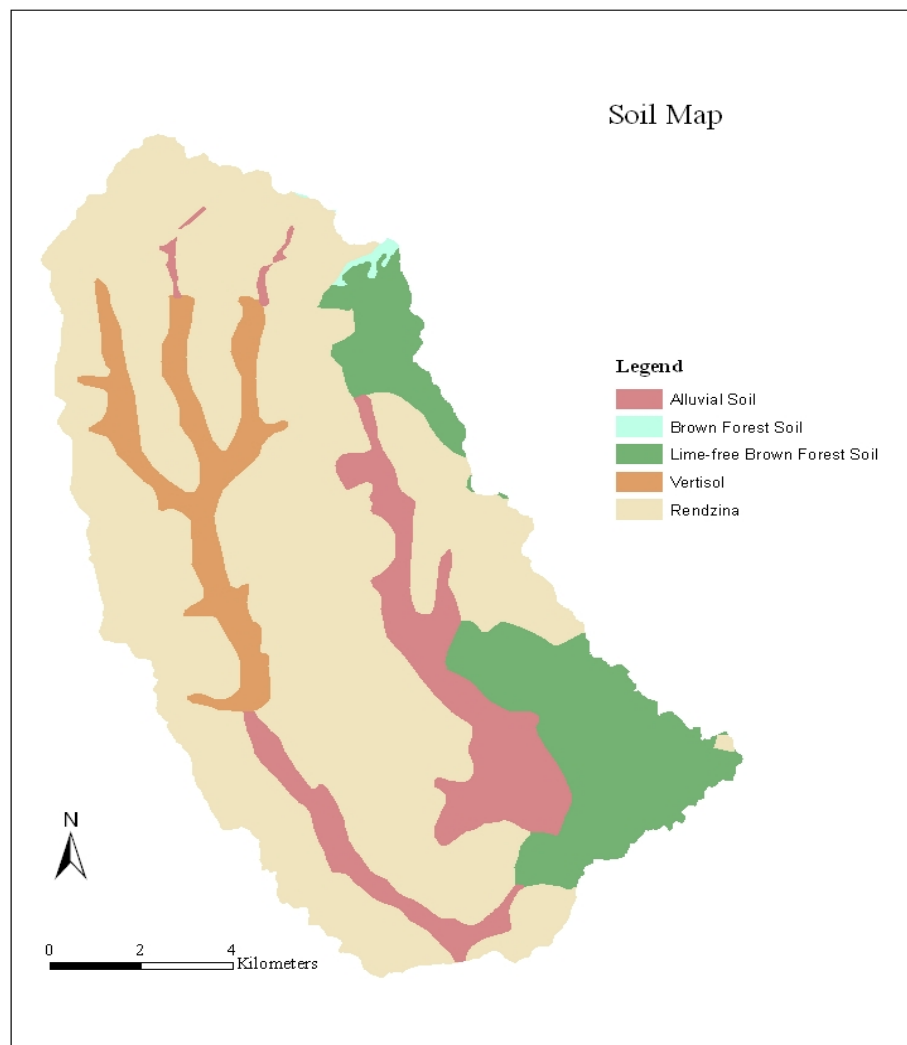


Figure 16: Soil map of the Sazlıdere watershed (taken from the General Directorate of Agricultural Research).

3.6.1 Water Erosion

Watershed characteristics, such geological factors including bedrock type, its permeability, the slope of the land, the condition and characteristic of soil within the catchment area, and climate together can contribute in varying degrees to the erosion process in the site. In this process, sediment and nutrients eroded from various land use activities within the catchment are carried to the reservoir. The transportation of these constituents to the reservoir can cause water-quality problems. Pollutants from soil erosion, farming fields, urban roads, and municipal facilities and construction activities can contribute to the problem of surface runoff during storm events.

The water erosion map of the Sazlıdere watershed (Figure 17) indicates three levels of erosion: none or slight, moderate, and severe. A large portion of the catchment is intensely eroded. The area is mostly used as dry farming land with no covered vegetation, and even the forested area is highly sloped. In the north of the basin, the area between the streams and low-lying areas is affected moderately by erosion. None or slightly eroded areas are generally found where the reservoir and large parts of the streams are found. The map indicates how water erosion plays an important role in the sediment and nutrient loading of the Sazlıdere reservoir. Storm water runoff coming from growing urban areas had a considerable impact on the loading of the reservoir.

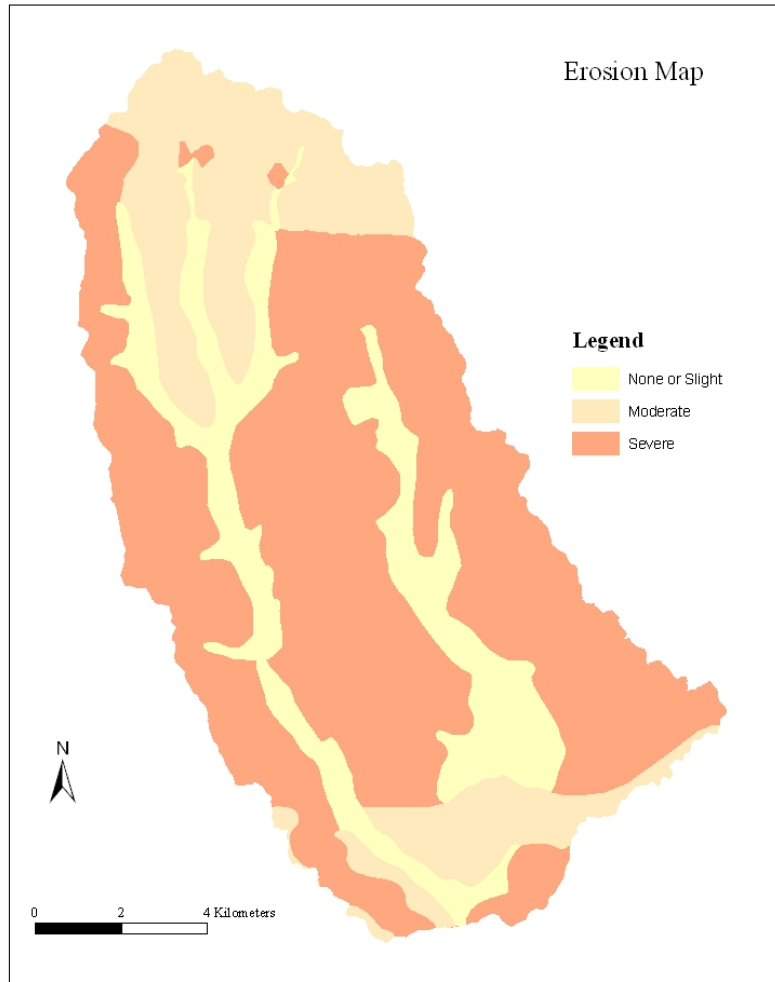


Figure 17: Map showing the degree of water erosion (taken from the General Directorate of Agricultural Research).

CHAPTER 4

MATERIALS AND METHODOLOGY

4.1 Introduction

The methodology of this research includes sections related to the preprocessing of satellite data, extraction of water spectral signatures, multiple regression analysis of ground measurements and corresponding water signatures. The preprocessing was carried out by rescaling raw radiance data provided by space sensors to surface reflectance using an atmospheric correction program and masking the study area by removing irrelevant data from the image scene. These procedures are followed by the extraction of water spectral signatures. In the next step, a statistical model is created to predict water quality variables using regression analyses between spectral signatures of sample sites extracted from the study area image and field measurements of the quality variables. Then, based on the predictive model the entire image was converted into water quality thematic maps. Thus the model determined the concentrations of water body constituents from satellite data, which was obtained by comparison of the actual measurements.

4.2 Data Collection

Three data sets were used in this study. These are satellite and ground observation data gathered from the Istanbul General Directorate of Water and Wastewater (ISKI), and atmospheric data gathered from the State Meteorological Administration.

4.2.1 Satellite Data

Four IKONOS satellite images were processed in this research. Each image consists of four multispectral bands. All images were geometrically corrected and registered according to the Universal Transverse Mercator (UTM), Zone 35 geographic projection using WGS84 datum by the satellite vendor. The root mean square error (RMSE) for positional accuracy was generally within 20 meters. All images used in this study were cloud free. The image processing was performed by Erdas Imagine, version 9.1. Information about satellite data is shown in Table 5.

TABLE 5: SATELLITE DATA USED IN THIS STUDY

Image Date	Bands		Map projection	File Format	Dynamic Range
5/30/2007 6/1/2008	Band 1 Blue:	0.45 - 0.53 micrometer	UTM/WG84	Geo Tiff	11 bit
	Band 2 Green:	0.52 - 0.61 micrometer			
	Band 3 Red:	0.64 - 0.72 micrometer			
	Band4Near Infrared:	0.77 - 0.88 micrometer			

4.2.2 Ground Observation Data

For this study, field observation data comprises four water quality variables obtained from the Istanbul General Directorate of Water and Wastewater (ISKI). These were secchi depth, chlorophyll-a, total suspended solids, and total phosphate values measured at six sample sites for each date. Five sample sites are located within the Sazlıdere reservoir image scene, and one sample site for 2007 and two sample sites for 2008 were used from an image scene of another reservoir adjacent to Sazlıdere, because in performing the regression analysis the number of ground

observations is required to be exceeding IKONOS four multispectral bands by two or more. Reservoirs were sampled in May 2007 and 2008 used in this study (Table 6). Ground observation data acquired within 10 days of the satellite overpass was used, except for one ground measurement in 2007 which was within 15 days. Image dates for IKONOS used in this study and available ground observations of water quality parameters within 10 days of the satellite overpass.

TABLE 6 : INFORMATION FOR GROUND OBSERVATION DATA

Number of Ground Measurements	Date	Water Quality Parameters
5	5/31/2007	SDT, Chl-a, TSS, TP
1	5/15/2007	
4	5/21/2008	
2	5/22/2008	

4.2.3 Atmospheric Data

The atmospheric data consist of rawinsonde observation data and visibility data obtained at two weather stations, in Goztepe and Kirecburnu, by the State Meteorological Administration.

The rawinsonde system is a radiosonde designed to take measurements of meteorological data including pressure, temperature, relative humidity, wind speed and direction. A radiosonde is a balloon-borne platform with instruments used to measure meteorological parameters while ascending through the atmosphere. (OFCM, 1997). Visibility is a measurement of transparency of air. It is usually reported within weather station observations.

The rawinsonde data measured for Goztepe station at 12:00 which is on the morning of the IKONOS image acquisition (May 30, 2007) were used. Weather

conditions on May 30, 2007 were very hot with clear sky. Similar visibility condition occurred on June 1, 2008. The atmospheric data are used to define an atmosphere model and visibility for ATCOR 2 inputs.

4.3 Image Preprocessing

The satellite imagery used in this study was processed in a standardized procedure which included atmospheric correction and the masking of unneeded features.

4.3.1 Atmospheric Correction

The aim of atmospheric correction is to convert raw radiance recorded by sensors to true ground reflectance by removing the effects of atmospheric and the solar illumination. Thus, quantitative biophysical parameters of reservoir water can be extracted from the satellite data.

IKONOS satellite data were converted to true reflectance values using ATCOR software. ATCOR version 9.1 was used as an add-on module of the ERDAS IMAGINE image processing package. ATCOR2 was employed for the image scenes consisting of the reservoir study area. Before performing the atmospheric correction process, the IKONOS four bands (blue, green, red, and infrared) are stacked in ERDAS IMAGINE to create a single input file to ATCOR2.

The atmospheric correction procedure was performed in sequential steps based on ATCOR2 requirements. The first step in the correction process is to define the input of data parameters. For the ATCOR2 input parameters, specifications including an acquisition date, a scale factor, sensors type, calibration file, the solar zenith, ground elevation, and atmospheric selection parameters consisting of scene visibility and the model for solar region were indicated correspondingly.

In the statement defining the input parameters, first the acquisition date and sensor type were specified using the IKONOS metadata file. The output scale factor was set to 10 from the default value of 4 which encodes the output image with reflectance value in the 8-bit to preserve the 16-bit range of IKONOS data.

The default calibration file in ATCOR provided for IKONOS was used. This file contains the calibration coefficients Bias (c0) and Gain (c1) for each band. ATCOR offers adopting those c0 and c1 values iteratively using the Spectra Module.

The Solar Zenith value which is referred to in ATCOR2 as the angle of the sun off-nadir was specified next. The solar zenith angle was calculated using the following equation:

$$\text{Solar Zenith (degrees)} = 90 - \text{Sun Angle Elevation} \quad (4.8)$$

The sun angle elevation values provided in the IKONOS metadata files were used. The results were processed as input values for ATCOR2.

The last input parameter is the average height ASL (Above Sea Level) for defining ground elevation was calculated from the Digital Elevation Model (DEM) where the image area is enclosed.

As one of the atmospheric selection parameters, scene visibility was set based on metrological information at the time of image acquisition. The next parameter is the model for the solar region corresponding to sensor tilt angle and direction, aerosol and atmosphere type. This was done in three steps.

The tilt angle pertaining to the angle of the sensor off-nadir was determined at the first step. The tilt angle in IKONOS metadata is defined as Nominal Collection Elevation. The tilt angle was calculated using following Equation.

$$\text{Tilt Angle (degrees)} = 90 - \text{Nominal Collection Elevation} \quad (4.9)$$

The tilt angle in ATCOR is defined as 0, 10, 20, and 30 degrees. The calculated tilt angle was rounded to the closest default angle.

The setting of the tilt direction of the image was determined at second step. The direction (N, S, and E, W) is defined by the relative azimuth between sensor line of sight (nominal collection azimuth of the sensor) and the solar azimuth. The azimuth was calculated using Equation 3.

$$\text{Relative Azimuth} = \text{Nominal Collection Azimuth} - \text{Solar Azimuth} \quad (4.10)$$

The Solar Azimuth can be found within the metadata like the Sun Angle Azimuth. Since ATCOR can only provide a relative azimuth of $0^\circ = S$, $30^\circ = E$, $120^\circ = N$, $150^\circ = W$, the calculated solar azimuth angle was rounded to the nearest defined angle to determine the direction.

The third step in setting the model for the solar region is to specify the aerosol and atmosphere type. As a type of aerosol the urban option was used, since study area is affected by urban and industrial aerosol sources. For atmosphere options, ATCOR2 provides six atmospheric models. To define the atmosphere model that is most similar to the default one, total water vapor content (0-5km) was calculate using metrological data during the image acquisition time. The total water vapor was calculated using the following equations (Sarıkaya, 2006).

$$e = (rH/100) * 0.6108 * \text{EXP}(17.27 * T) / (T + 237.3) \quad (4.11)$$

Where e is ambient vapor pressure in kPa, rH is relative humidity as percentage , T is temprature in degrees Celsius

$$\rho_v = 0.622 * e / (R_g * T) \quad (4.12)$$

Where ρ_v is vapor density in g / cm², R_g is gas constant for dry air ($R_g=2870$)

$$u_i = h_i * (\rho_{vi} + \rho_{vi+1}) / 2 \text{ (linear change in } \rho_v) \quad (4. 13)$$

Where u_i is water vapor in each altitude observation. Change in water vapor was assumed linearly.

$$\text{Total water vapor: } u = \rho_v * h \text{ (0-5km altitude)} \quad (4. 14)$$

The measured water vapor profile was selected according to the closest default atmospheric model. The calculation of water vapor was done only for the images acquired in 2007. For the images in 2008, an atmospheric model was assumed in the same as 2007.

After all input parameters in ATCOR2 were entered, the validate spectra module was used next. The spectra module enables one to verify if the calibration file is correct. ATCOR states the IKONOS default calibration file cannot give correct results in some cases. An auto-calibration option was used to adjust the default calibration file. The spectra of a known target measured from the images were compared to reference spectra provided in the ATCOR library. Thus a new calibration file was written automatically. Once the calibration file was adjusted with its spectra module, atmospheric correction was processed. The output DNs represent percent of reflectance scaled by a factor for reflectance. To obtain the true reflectance for a certain pixel, ATCOR recommends dividing output pixels by a defined scale factor value. Thus, the output pixel was divided by 10 using the Spatial Modeler in ERDAS Imagine.

4.4 Extraction of Reservoir Water Image

This step covers the extracting of the reservoir water image. As only reservoir water area is needed for this study terrestrial and other unneeded areas were removed from the image scenes. This procedure helps both reducing file size and processing time of the images. To differentiate water from terrestrial areas an unsupervised classification method was performed on the images. This simpler method in contrast to a supervised classification method is successful in identifying water pixels (Zhang, 2008). All images were classified into 10 classes using the ERDAS unsupervised classification option. Then a mask was created to extract only the water classes from the original image. This step was processed using the Imagine mask option. The unsupervised classification image was used as an input mask file. All terrestrial classes were set to 0, while water classes were assigned to 1 using the recode button. After water classes were extracted, only the study area was taken out from other unneeded areas, cropped using an Area of Interest (AOI) and the subset option in ERDAS.

4.5 Derivation of Water Spectral Signatures

The spectral data from the images were extracted at each sample site location using the following procedure. First, each point corresponding to the field measurements were selected using the AOI tool of ERDAS. All AOIs were enclosed using the rectangle selection tool. Then the AOIs consisting of a 3*3 pixel window centered on sample points were created at all sample stations. Then, every AOI was activated, and in the Signature Editor, the “create new signatures from AOI” option

was selected. Each signature class was labeled according to the ID of sample locations.

After all reservoir signatures were acquired, these values were then averaged for each sample point using the columns properties/statistics option. The averaged signatures values for all bands and ID classes were selected, and then exported to a data file for further statistical analyses.

4.6 Multiple Regression Analysis and its Validation Using Jackknife Resampling

This process includes linear regression analysis between satellite reflectance and ground reference data for establishing predictive models of water quality parameters and the testing of coefficients of linear regression models using the jackknife resampling method to assess the validity of linear regression results. The jackknife procedure for validating data is especially useful when dealing with a small sample size (McGarigal et al, 2002). In jackknife, subsets of statistics for fixed data sets are recalculated (Shao and Tu, 1995). In order to find the bias of these statistics, the average of these statistics is compared with corresponding statistic of the entire sample. In this way the bias is estimated. The jackknife procedure may be used to help estimate and then reduce biases in the estimators (Mooney and Duval, 1993).

For the regression analysis procedure, the relationship between ground measurements and the spectral response of reservoir water extracted at each sample site location mentioned in the initial section for the visible and near-infrared bands of IKONOS was quantified through a linear statistical model. Multiple linear regression analysis tool in Excel was used to quantify the relationship between these data and

create a model based on regression coefficients to predict water quality parameters over the whole reservoir. The values of dependent variables (secchi depth, chlorophyll-a, total suspended solids and total phosphate) and independent variables (IKONOS bands) were used to estimate the model coefficients.

Regression analysis was employed for the relationship between the SDT and IK3:IK1 ratio, along with IK1. The band combination of IK3:IK1 ratio, along with IK1 was selected since previous studies found it to be a strong predictor of SDT (e.g., Olmanson et al, 2008; Sawaya et al, 2003). Regression analysis of Chl-a, TSS and TP were calculated for their relationship with bands of IK1, IK2, IK3 and IK4. This model is based on the general form of the linear regression equation which has been adopted to determine water quality parameters (Sarikaya, 2006).

First the output files of spectral signatures and observation data were imported into an Excel spreadsheet. The satellite reflectance IK1:IK3 ratio was calculated first for secchi disk depth. The multiple regression analysis was performed using SDT as a dependent variable and the IK1:IK3 ratio, along with IK1 as independent variables. Besides this, the Regression analysis of other water quality parameters including chlorophyll a, total suspended matter and phosphorus were performed with ground observation of each parameter as dependent variables and four bands of IKONOS as independent variables.

The regression models used in this study are:

$$WQ(\text{Chl-a, SSM, TP})=a + b(\text{Band1})+c(\text{Band2})+d(\text{Band3})+e(\text{Band4}) \quad (4. 15)$$

$$(\text{SDT}) =a + b (\text{Band1}/\text{Band3}) +c (\text{Band1}) \quad (4. 16)$$

Where a, b, c, d are coefficients from regression analysis.

The coefficients for each parameter were obtained; the models were applied to reservoir water images using Spatial Modeler in ERDAS IMAGINE.

To assess the validity of regression models, data used in these statistics were applied for the jackknife resampling method in SYSTAT. The jackknife sampling estimates of the regression coefficients were correlated with ground measurements of water quality parameters to produce the validation R², and then graphs of correlation were generated using Excel.

4.7 Water Quality Maps

Thematic maps of each water quality parameter were generated from the regression models. Once the models were applied to each individual water pixel using a modeler, the results were imported into ArcView 8.7 to create a pixel-level reservoir map. In the ArcView Legend Editor, a graduated color legend type was selected. The legend was classified according to Carlson's Trophic State Index showing the Secchi, chlorophyll-a, and phosphorus measurements. TSI characterizes the level of lake biological productivity ranging from 0 (oligotrophic) to 100 (hypereutrophic). Trophic condition maps were created for each and other thematic maps are shown in Figures 18, 19, 20 and 21.

CHAPTER 5

RESULTS AND CONCLUSIONS

5.1 Introduction

The purpose of this chapter is to describe the results and implications of this study and to discuss them. Also, this chapter will present the major conclusions and limitations of this study and recommendations for further research.

The results section will initially focus on the evaluating of the statistical relationship between IKONOS bands and ground measurements, carried out by multiple regression analysis developed for predictive models to quantify the water quality parameters throughout the reservoir. Furthermore, the reservoir water quality will be assessed based on thematic maps of spatial and temporal distribution of suspended sediment concentrations and trophic state indicators which is categorized according to Carlson`s TSI. The discussion will provide a description of the synthesis of the findings through a focus on spatial and temporal variations of trophic conditions associated with total phosphorus, chlorophyll-a and Secchi Disc Transparency relationships and suspended sediment concentration in the reservoir, and inferences of the effects of land use on reservoir water quality.

The conclusion section of this thesis will represent a broad spectrum of the main results and show the significance of the results, describe the main limitations experienced in the study, and suggest some future research based on these findings and the limitations of this research.

5.2 Results and Discussions

5.2.1 Regression Analysis

The predictive models derived from regression analysis of all data set were evaluated based on the coefficient of determination (R^2) of regression analysis and the correlation between actual ground measurements and predicted values of water quality parameters obtained from the jackknife resampling method. The R-squared values have primary importance since the purpose of the regression analysis is to create a model that predicts the water quality variables making accurate predictions. Thus in the regression assessments R-squared was primarily considered. The performing of the regression analysis showed a generally strong relationship between IKONOS bands and ground measurements of water quality parameters. Based on results from regression analysis the models used for SDT, Chl-a, TP and TSS produced a commonly high correlation between ground measurements of those and corresponding reflectance in bands, with R^2 ranging from 0.65 to 0.98. Although the models based on regression analysis have generally showed a satisfactory performance in their estimates of water quality parameters (SDT, Chl-a, TP and TSS), results from the jackknife resampling method indicated successful prediction of SDT and TSS, but low accuracy for Chl-a and TP.

After all predicted values of water quality variables were represented as a series of thematic maps, the predictive success of models were evaluated visually by comparison with ground measurements and the satellite image. The models generally produced results that remained consistent, except the model used to estimate water clarity in 2007. While the correlation coefficients of the model were high ($R^2=0.83$)

and the model performance based on the jackknife resampling method was R^2 of 0.62, the model overestimated SD values when the clarity was low. This might be because the data set used to develop the model mostly was distributed over a narrow range. As an alternative, the model used for other parameters was applied to the SDT data to predict SDT for 2007. The new model for SDT consistently performed better in the same data set. The bands used in this model seem to be better able to show detailed optical characteristics of water and materials in water.

5.2.2 Spatial and Temporal Variations of Water Quality Parameters

Temporal changes of water quality parameters from thematic maps for May 30, 2007 and June 1, 2008 were evaluated by comparing ground observations and visual interpretations of satellite images. The data sets generally showed consistent tendencies. In other words, the same trend of variations between satellite estimated and ground observed water quality parameters were shown. Moreover thematic maps exhibited more details of spatial and temporal variations of quality parameters over the whole reservoir than ground data. A synoptic overview and clear differentiation of temporal and spatial distributions of quality parameters from thematic maps showed potential for the detailed features to design or improve ground sampling strategies through marking optimal water sample site locations.

Spatial variations of reservoir water quality in 2007 (Figure 18) showed that chlorophyll-a was highest in the southeastern side and northwestern end of the reservoir and decreased towards the central part. The majority of the reservoir, mostly the central part was characterized as eutrophic, while the southeastern end showed hypereutrophic conditions, and the northwestern end of the reservoir indicated upper eutrophic levels.

In 2008, Chl-a was highest in the northwestern end and most of the central part of the reservoir, which is represented by eutrophic conditions, as Chl-a was low in the southeastern side and some parts from northwestern towards to central of the reservoir, it was characterized as oligotrophic.

The comparing of the thematic maps of water quality parameters for May 30, 2007 and June 1, 2008 from the early summer periods allowed for visibility of the direct effect of climate regime on water quality. For instance the distribution of chlorophyll a concentration indicated Chl-a in 2007 was higher than Chl-a 2008. This can be explained by less nutrients loading during 2008. According to TSI, the southeastern side of reservoir indicated oligotrophic conditions in 2008, while it identified eutrophic conditions in 2007. This could be because in 2008 water flow from this portion of the reservoir was blocked; this might have led to the area not having water drawdown conditions. Also in 2007, water levels at this southeastern part of reservoir fell, possibly causing less dilution of pollutants. The spatial variability within the reservoir for Chl-a in 2008 is more than 2007, while the majority of reservoir indicated eutrophic conditions at the both periods.

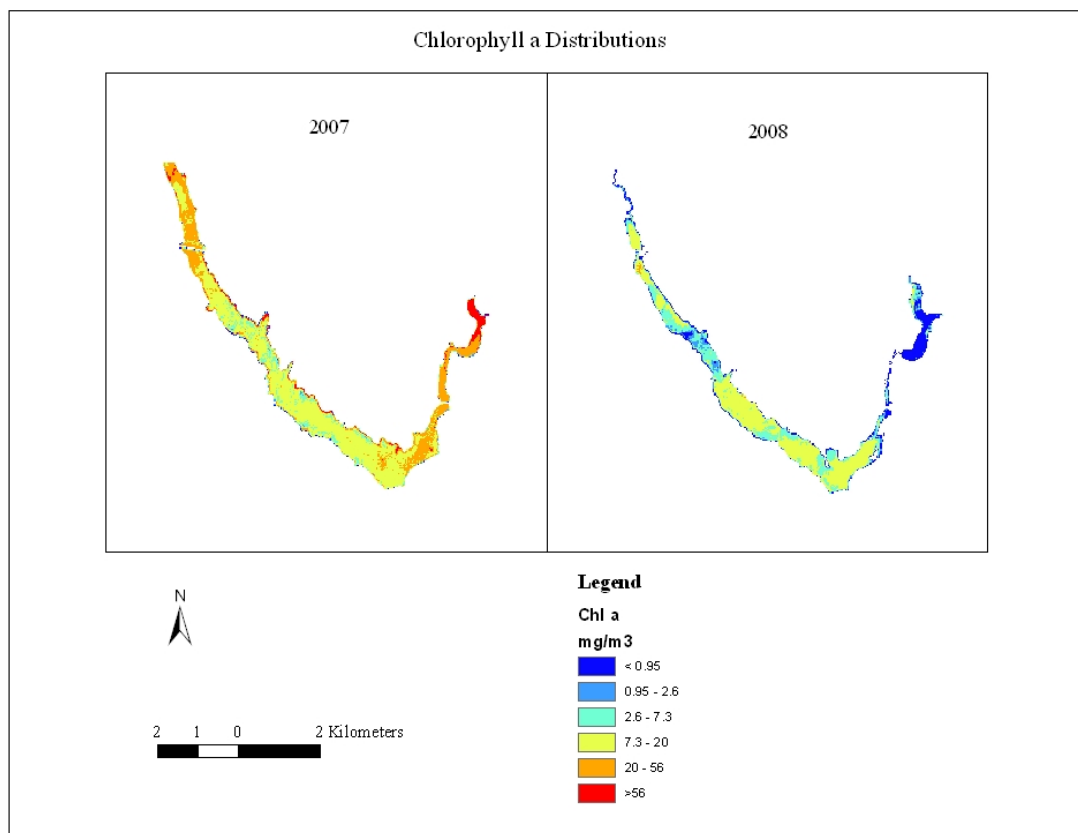


Figure 18: The distribution of Chl-a concentration in 2007 - 2008.

The distribution of total phosphate concentration for 2007 indicated the whole reservoir was characterized by eutrophic conditions of phosphate except the southern section which indicated hypereutrophic levels. If viewed according to eutrophic level differences, it can be seen that an upper level of eutrophy occurred from the northwestern and southeastern ends towards to central of the reservoir. In 2008, the reservoir could have received internal phosphorus loading rather than external loading; the total phosphate level may have been strongly influenced by resuspended sediment caused with wind induced waves. With a decrease in the water level and the occurrence of resuspension, phosphate levels remained mesotrophic in the majority of the reservoir and eutrophic at some parts of the central area. There is an exception

to in the northwestern end of the reservoir, which showed oligotrophic level. Furthermore results of TP concentrations indicated that the variations in TP followed the same trends of chlorophyll a for 2007 and 2008. This appeared to support the idea that increased nutrient loading frequently results in increased algal biomass.

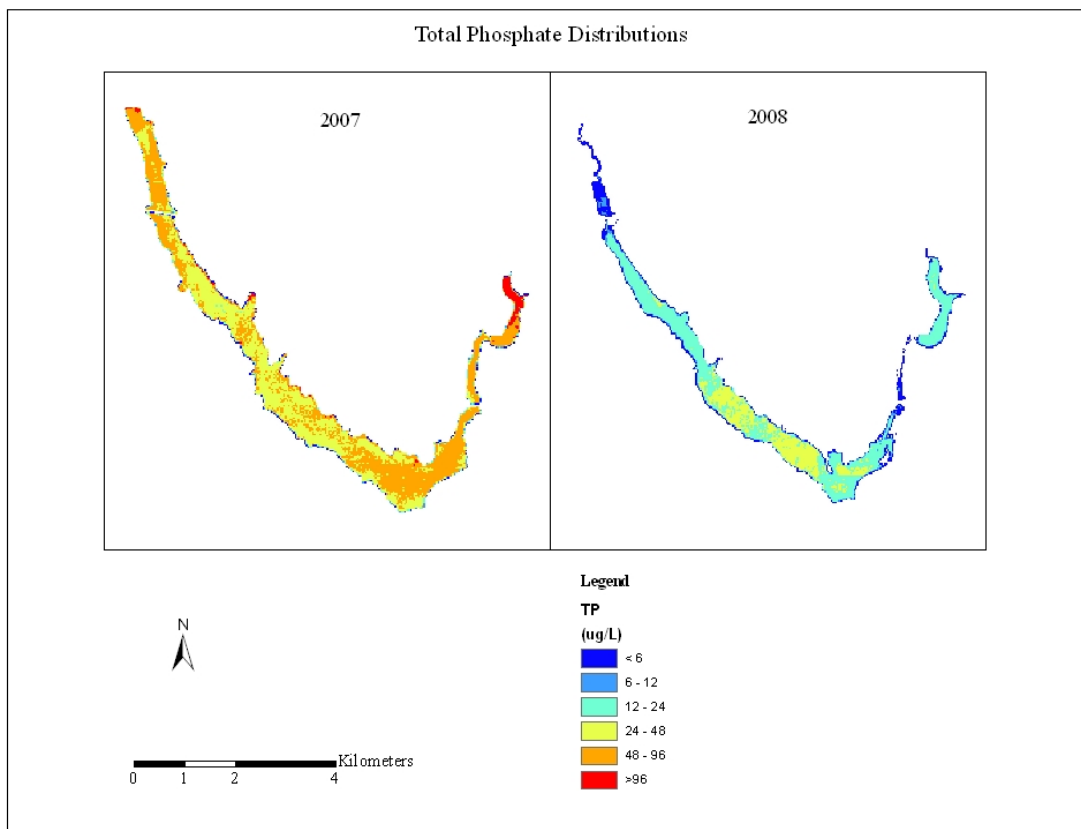


Figure 19: The distribution of TP concentration in 2007 - 2008.

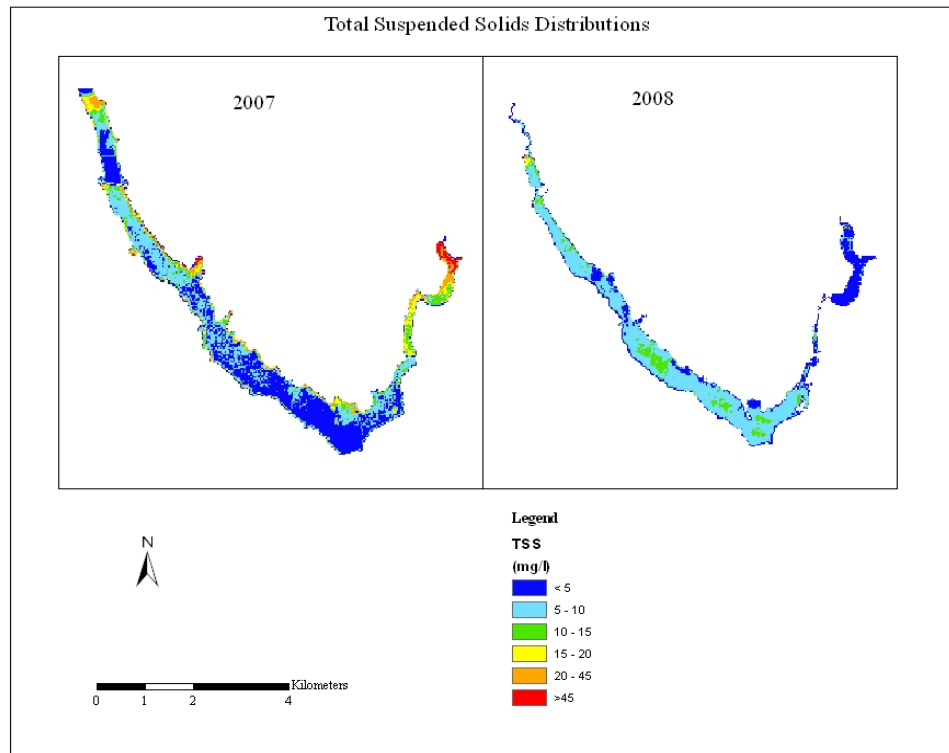


Figure 20: The distribution of TSS concentration in 2007 – 2008.

The spatial variations of suspended sediment for 2007 showed that high TSS concentrations appeared in the southeastern extension of the reservoir where the water level is lowest. The southern part of the reservoir has low levels of sediment. Moving from the southern part towards the northwest, sediment levels increase. There are also two areas of low sediment in the northwest section of the reservoir. It seems that sediment levels are related to the water level or shallowness of the reservoir. In 2008 there was a general increase in sediment. This is due to resuspension of sediment due to a lower water level. The exception to this trend is in the eastern section of the reservoir. Here the water flow was blocked, allowing water increase in the eastern section.

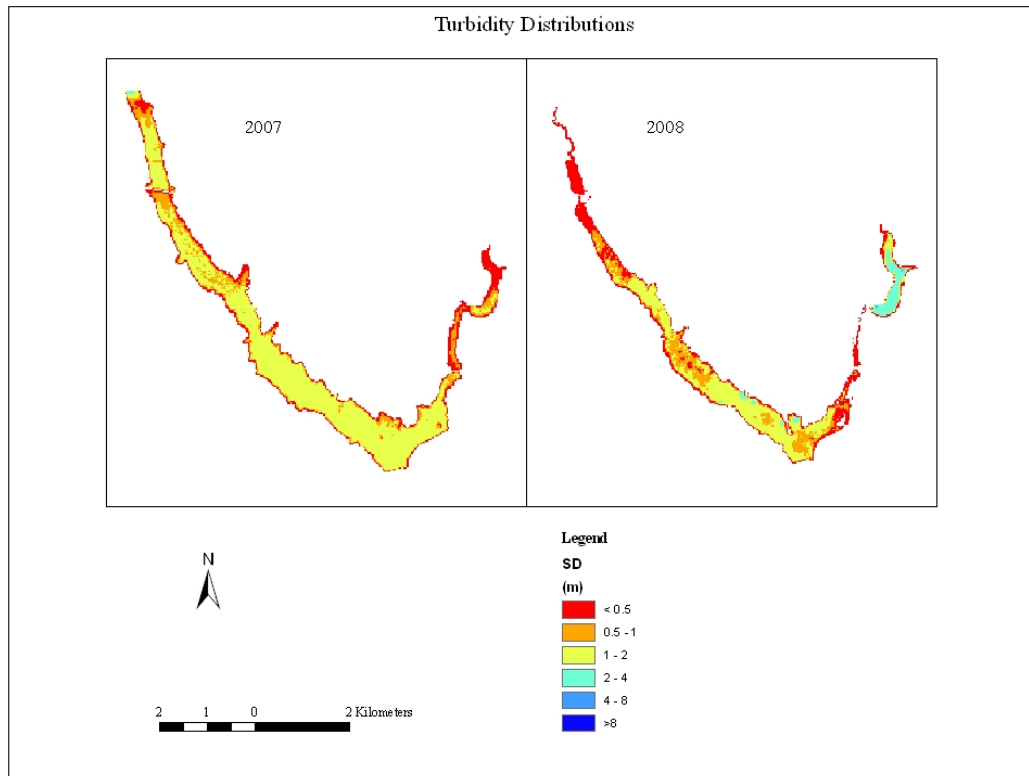


Figure 21: The distribution of turbidity (SDT) in 2007 and 2008.

The spatial distribution of Secchi disk depth from thematic maps exhibited that SDT was relatively uniform towards central of the reservoir in 2007, which was largely characterized as eutrophic. It decreased towards the southeastern portion and some areas in the northwestern part of the reservoir, which indicated hypertrophic conditions. In 2008, due to low water levels or the shallowness of the reservoir, SDT generally decreased across the reservoir with the exception of at the southeastern section. This section showed mesotrophic conditions apart from the end stripe of it. The northwestern section of the reservoir indicated hypertrophic levels. The upper level eutrophic conditions occurred towards the central area.

5.2.3 Land use and water quality

The thematic maps of water quality indicators have been used to assess the effects of surrounding land use on the reservoir's water quality based on spatial and temporal patterns. Comparing maps from the same date at different years showed that there was a large water level decrease in 2008 which appeared in viewing that some streams that normally reach the reservoir were almost disconnected from the main water body. This was the result of an extended drought period. This showed that lower TP and Chl-a loads in 2008 can be explained by less nutrient loading occurring due to extended dry periods. This also can suggest that most amounts of nutrients discharged during high water flows from the watershed land area. Since a large portion of the catchment is exposed intense water erosion, especially the area which largely used for dry farming. Thus the sediment and nutrients from agricultural land and urbanized land through storm runoff are carried to the reservoir during high rainfall events.

5.3 Conclusions

The procedure of quantification of water quality parameters from satellite data was successfully established. The statistical relationships between satellite data and water quality variables were calculated to construct a model for the quantification of each parameter using different band combinations. Predictive empirical models using linear regression analysis were successfully developed. Although linear regression analysis produced strong relationships between ground measurements of water quality parameters and corresponding IKONOS reflectance data, the jackknife resampling method used for those statistics showed a bias in the regression estimates

obtained for the models of Chl-a and TP. The results of the jackknife resampling method have determined that the performance of the model used for estimating Chl-a and TP is low, and that for the model estimating SDT and TSS is high.

The results from models of variables showed that the IKONOS four bands setting produced higher accuracy than the model with the band setting of IK1:IK3, along IK1 when applied for the same data set of SDT measurements. This may be due to the wider range of the bands, which made it possible to reveal details of changes in parameters optical characteristics.

IKONOS satellite data have been successfully used for the quantification and mapping of suspended sediment, chlorophyll-a, total phosphate, secchi disk depth distributions. Due to the capability of providing high spatial details and synoptic views of the water quality parameters and watershed characteristics, satellite data have enabled valuable information in the assessments of water quality covering the entire water body of the reservoir. The satellite-derived thematic maps enabled the visualization of spatial and temporal variations of the parameters. Also, visualized results showed great potential for the rapid understanding of the progression of water quality conditions by providing high spatial details and continuous spatial coverage over the reservoir, which could be useful for conservation planning for the reservoir. Furthermore both imagery and thematic maps providing clear visual differentiation on the patterns of distribution of water quality parameters have demonstrated potential to be used as a guide to locate the areas where ground measurements would be the most useful.

Using satellite data from near similar dates in different years provided the valuable opportunity for detection of change in water quality variables. Temporal

variations from both dates of an early summer index period demonstrated that reservoir water level and shallowness are important factors affecting water quality. Use of anniversary dates also indicated that variation or extremity in climate can lead to alterations of temporal patterns of the reservoir's water quality variables and showed the potential of temporal records in understanding variations in the reservoir's water quality.

Spatial and temporal patterns of distribution of Chl a, TSS, TP and SDT demonstrated that variations in the water quality generally occur in the northwestern and southeastern portion of reservoir. Also it continues towards the central part of the reservoir. The spatial and temporal variations in water quality at different sites of the reservoir can be explained by reservoir shallowness, decreasing water volume and depth, and sediment resuspension events. Moreover variations in water turbidity largely were influenced by water levels.

The reservoir's trophic status was clearly illustrated by thematic maps which were categorized according to Carlson's Trophic State Index. The assessment of trophic status was based on chlorophyll a, TP concentration, and Secchi Disc Transparency. The TSI for the three parameters have shown that relationships between indicators were interconnected in 2007. In general, the reservoir was characterized largely by eutrophic conditions. In 2008, TSI relationships between the quality indicators were not straightforward, since the parameters were lumped into different trophic classes. The reservoir's trophic status generally varied between mesotrophic and eutrophic conditions

Investigating the impacts of land use in reservoir water quality showed that there was no direct proof of any spatial or temporal trend in the water quality parameters to

evaluate the effects of land use on reservoir water quality. Nevertheless the lower water level during 2008 resulted in less nutrient loading into the reservoir. It may be inferred from this that nutrient loading from the surrounding area increases during high runoff events. Since the most of the catchment areas are exposed to intense water erosion, this can show evidence of association with nutrient loading, especially from agricultural land and the combined sewer system in the urban areas, which can quickly be washed from the catchment to streams during runoff events.

5.3.1 Limitations of the Study

There were several limitations that need to be acknowledged regarding the present study.

One of the limitations is that a sufficient number of ground reference measurements were not available for the study area to develop a regression analysis. This lack of data may result in uncertainty in regression analysis. This is due to the fact that the small sample used is not sufficient to show that the results are not only due to chance. In this study, due to the unavailability of a sufficient sample size, a limited number of ground reference measurements from an adjacent IKONOS scene which involves a time difference between satellite overpass and concurrent ground reference sampling were employed. The use of data like in this case may affect the accuracy of the results with respect to the regression analysis, as water quality parameters can reveal short-term variability.

The lack of bathymetric data restricted attempts at evaluating the findings regarding spatial and temporal patterns in reservoir water quality variables. This data, when used in conjunction with thematic maps representing the distribution of water

quality parameters can provide a comprehensive assessment. The findings discussed within the context of spatial patterns in quality parameters under drawdown conditions could benefit from a level contour map describing the bathymetry within the reservoir.

Another limitation concerns the variety of time periods of data used in this study. The amount of time series satellite data available was not enough to make it possible to evaluate variations of reservoir water quality. The temporal and spatial patterns of the water quality of the reservoir were restricted to being examined by comparing only the findings from two satellite data sources. Multi-date satellite images are required to improve the understanding of spatial and temporal patterns in the reservoir water quality.

5.3.2 Future research

Based on the findings and limitations of this present study, the following implications for further research are recommended:

1. Remote sensing data from multi-time series and different platforms should be employed to improve the understanding of the spatial and temporal patterns of the reservoir water quality and satellite-based observations. Multi-time series data can be used to indicate seasonal variations and trends in water quality over time. These data also can be used to detect the sources of pollutants being discharged into the reservoir by attempting to relate spatial and temporal variations in water quality parameters to the land use type or to a specific location within the watershed.

2. More ground reference samples should be employed to develop a regression relationship between satellite data and ground measurements. Ground sample points

should be distributed over a wide range in water quality to enhance accuracy of the empirical method.

3. Different methods (semi-empirical, analytical) used to estimate the concentrations of constituents in water should be employed to establish the best predictive model to quantify water quality variables throughout the reservoir.

4. Concurrent ground reference data with satellite overpasses should be collected to increase the accuracy of correlations between water quality variables and corresponding satellite data. Bio-chemical reactions in water can cause short-term variations of water quality parameters.

5. Different band combinations can be applied through stepwise regression analysis to reveal the best fit of algorithms to the optical characteristics of water quality variables.

APPENDICES

Appendix 1: IKONOS Image Metadata (2007 -2008)

Sensor: IKONOS-2
Acquisition Date/Time: 2007-05-30 09:07 GMT
Map Projection: Universal Transverse Mercator
UTM Specific Parameters
Hemisphere: N
Zone Number: 35
Datum: WGS84
DRA Applied: No
Nominal Collection Azimuth: 190.0456 degrees
Nominal Collection Elevation: 72.47926 degrees
Sun Angle Azimuth: 144.1283 degrees
Sun Angle Elevation: 67.46674 degrees
Percent Cloud Cover: 0

Sensor: IKONOS-2
Acquisition Date/Time: 2008-06-01 09:12 GMT
Map Projection: Universal Transverse Mercator
UTM Specific Parameters
Hemisphere: N
Zone Number: 35
Datum: WGS84
DRA Applied: No
Nominal Collection Azimuth: 231.4092 degrees
Nominal Collection Elevation: 71.84650 degrees
Sun Angle Azimuth: 146.2342 degrees
Sun Angle Elevation: 68.31841 degrees
Percent Cloud Cover: 0

Appendix 2: Atcor Inputs for IKONOS Image (2007-2008)

Acquisition date	30/ 5 /2007
Factor for reflectance	10
Sensor	IKONOS 2
Solar zenith	23.0
Ground elevation	0.1 km
Scene visibility	20 km
The tilt angle and the direction relative azimuth	20 E
Atmosphere type and aerosols	US standard urban

Acquisition date	01 /6 /2008
Factor for reflectance	10
Sensor	IKONOS 2
Solar zenith	22.0
Ground elevation	0.1 km
Scene visibility	20 km
The tilt angle and the direction relative azimuth	20 N
Atmosphere type and aerosols	US standard urban

Appendix 3: IKONOS Bands Used in the Regression Analysis (2007-2008)

Image radiance values per four IKONOS bands (2007)				
Station ID	Band 1	Band 2	Band 3	Band 4
S1	4.3	4.6	2.3	3.1
S2	4.8	5.2	2.3	3.2
S3	5.4	5.7	2.7	3.3
S4	3.5	3.9	1.5	1.8
S5	2.8	3.2	0.9	2.0
A5	2.9	3.9	1.5	1.7

Image radiance values per four IKONOS bands (2008)					
Station ID	Band 1	Band 2	Band 3	Band 4	Band1/band3
s2	4.7	6.4	4.4	5.9	1.1
s3	5.2	7.2	4.5	5.6	1.2
s4	4.6	7.2	4.1	5.5	1.1
s5	4.2	6.8	3.9	5.3	1.1
a4	4.1	5.8	3.3	4.3	1.3
a5	3.3	5.7	2.8	3.9	1.2

Appendix 4: Ground Reference Measurements Used in the Regression Analysis (2007-2008)

Water Samples (2007)				
Station ID	Chl-a (ug/L)	SDT(m)	TSS (mg/L)	TP(ug/L)
S1	33.9	1.0	7.20	60
S2	4.3	1.0	5.90	50
S3	16.5	1.3	6.30	40
S4	26.8	1.1	5.80	70
S5	17.9	1.1	4.60	40
A5	28.5	0.6	15.68	50

Appendix 4 continued.

Water Samples (2008)				
Station ID	Chl-a (ug/L)	SDT(m)	TSS (mg/L)	TP(ug/L)
s2	4.37	60	8.8	18.67
s3	10.18	60	8	23.67
s4	10.85	60	8.2	22
s5	9.17	80	6.6	22
a4	7.25	120	3.5	26.67
a5	5.39	180	2.6	20

Appendix 5: Regression Models and their Coefficient of Determination $s(R^2)$, and Models Performances based on Jackknife resampling method (2007-2008).

MODEL (2007)	Model R²	Validation R²
Chl-a = (105.7142476 + (2.366940604 * Band1) + (-38.8175267 * Band2) + (60.69239046 * Band3) + (-14.66501838 * Band4)	0.86	0.28
SDT = (0.796236754 + (1.035303168 * Band1) + (-0.580808077 * Band2) + (-0.516815667 * Band3) + (-0.131467655* Band4)	0.94	0.81
TSS = (7.271955129 + (- 18.08590573 * Band 1 + (12.39061183 * Band2) + (10.35009362 * Band3) + (-1.03025146 * Band4)	0.99	0.98
TP = (136.4809669 + (30.68593847 * Band1) + (-54.90929308 * Band2) + (55.90945288 * Band3) + (-27.37176503 *Band4)	0.74	0.01

Appendix 5 continued

MODEL (2008)	Model R²	Validation R²
Chl-a = (-19.01697254+ (2.13682105 * Band1) + (6.229569819 * Band2) + (-3.080494635 * Band3 + (-2.217168008 * Band4)	0.93	0.12
SDT = (1.318441374 + (2.023716651 * Band1/Band3) + (-0.619208368 * Band1)	0.90	0.95
TSS = (-14.18845856 + (1.118579542 * Band1) + (0.634661691 * Band2) + (-3.102288939 * Band3) + (4.583804051 * Band4)	0.99	0.89
TP = (12.18197685 + (9.767662706 * Band1) + (1.653009553 * Band2) + (-9.770419614 * Band3) + (-1.18848461 * Band4)	0.65	0.02

Appendix 6: Coefficients of Linear Regression Models and Jackknife Sampling Estimates of the Regression Coefficients, and Biases (2007-2008).

CHI-a (2007)			
	Coefficients	Jackknife Estimate	Bias
Constant	105.714	195.668	-89.954
BAND 1	2.367	306.989	309.356
BAND 2	-38.818	120.695	-159.513
BAND 3	60.692	227.852	-167.16
BAND 4	-14.665	43.293	-57.958

SDT (2007)			
	Coefficients	Jackknife Estimate	Bias
Constant	0.796	2.018	-1.222
BAND 1	1.035	-3.168	4.203
BAND 2	-0.581	1.586	-2.167
BAND 3	-0.517	1.754	-2.271
BAND 4	-0.131	0.656	-0.787

TSS (2007)			
	Coefficients	Jackknife Estimate	Bias
Constant	-14.188	-17.08	2.892
BAND 1	1.119	0.434	0.685
BAND 2	0.635	0.649	-0.014
BAND 3	-3.102	3.056	-6.158
BAND 4	4.584	1.308	3.276

Appendix 6 continued

TP (2007)			
	Coefficients	Jackknife	Bias
		Estimate	
Constant	136.481	1.156	135.325
BAND 1	30.686	496.077	-465.392
BAND 2	-54.909	-294.878	239.969
BAND 3	55.909	-195.564	251.474
BAND 4	-27.372	-114.562	87.191

Chl-a (2008)			
	Coefficients	Jackknife	Bias
		Estimate	
Constant	-19.017	-11.643	-7.374
BAND 1	2.137	3.883	-1.747
BAND 2	6.230	6.193	0.037
BAND 3	-3.080	-18.783	15.702
BAND 4	-2.217	6.135	-8.352

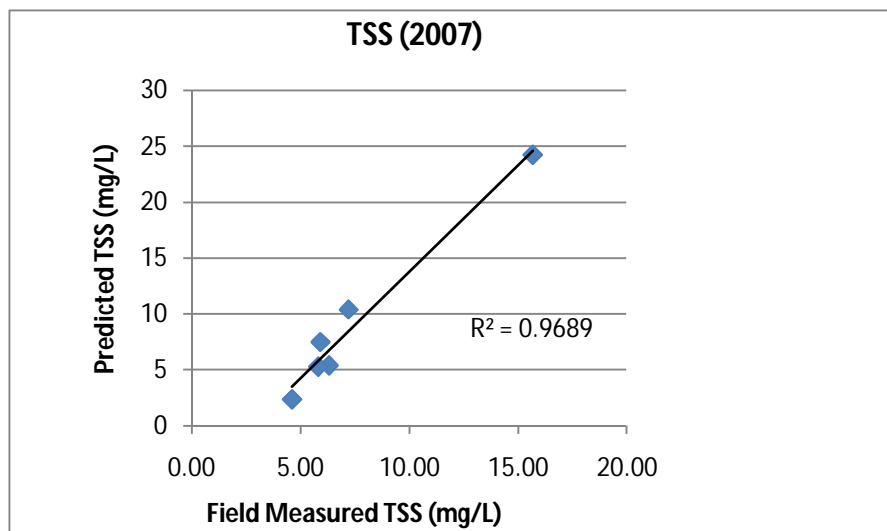
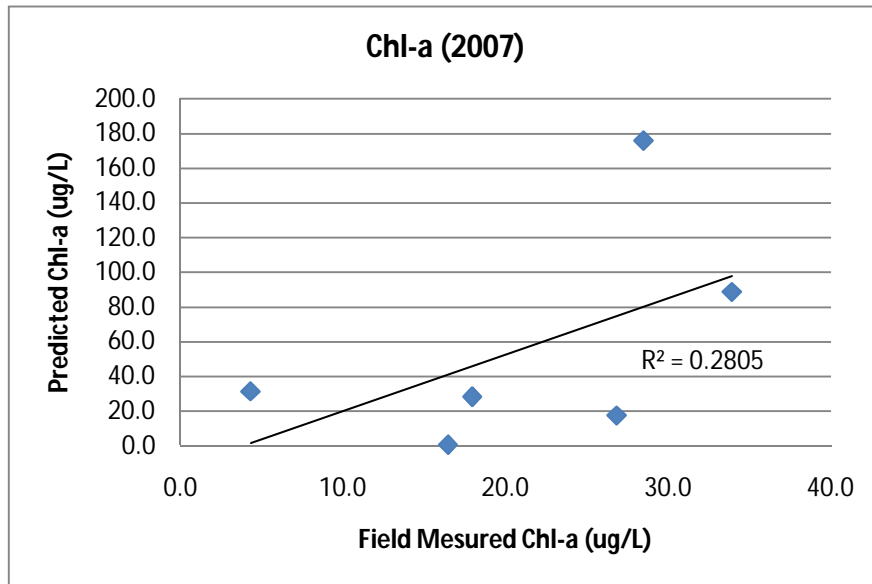
SDT (2008)			
	Coefficients	Jackknife	Bias
		Estimate	
Constant	1.3184414	2.275	-0.956
BAND1/BAND3	2.0237167	1.352	0.672
BAND 1	-0.619208	-0.656	0.037

Appendix 6 continued

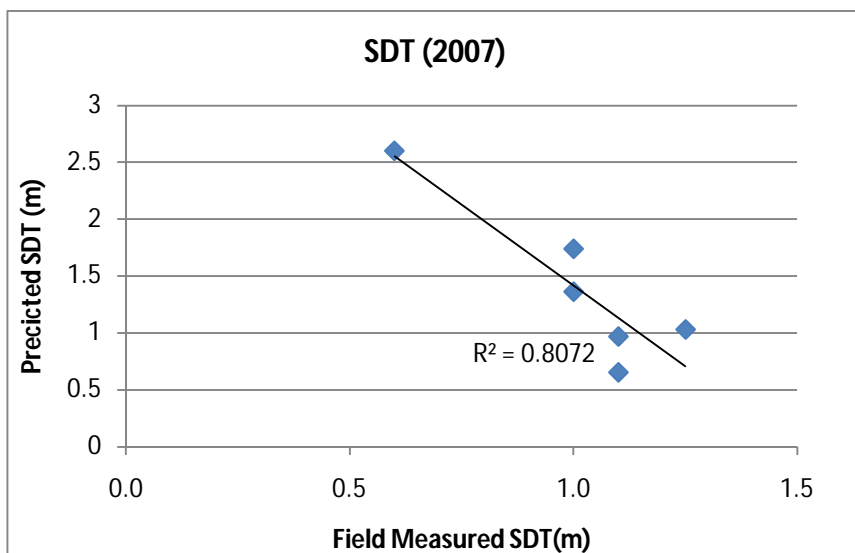
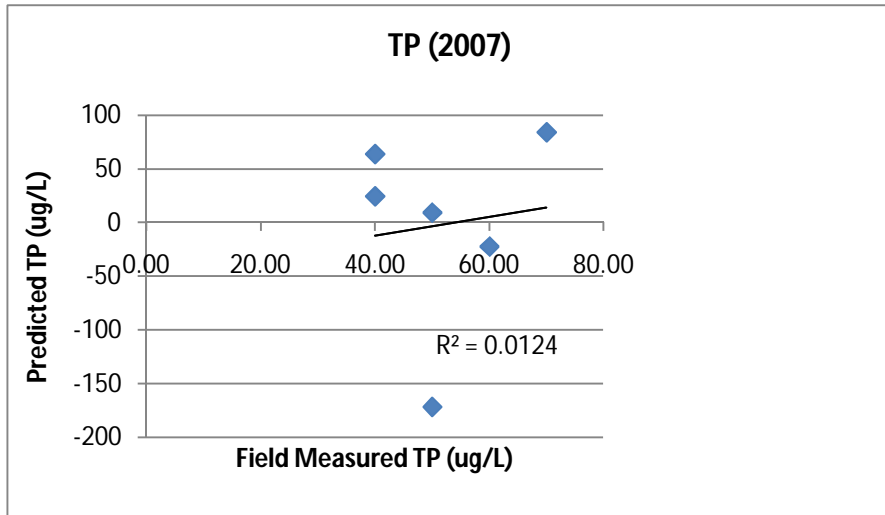
TSS (2008)			
	Coefficients	Jackknife	Bias
		Estimate	
Constant	7.272	12.507	-5.236
BAND 1	-18.086	-36.091	18.005
BAND 2	12.391	21.675	-9.284
BAND 3	10.350	20.079	-9.729
BAND 4	-1.030	2.343	-3.373

TP (2008)			
	Coefficients	Jackknife	Bias
		Estimate	
Constant	12.182	30.611	-18.429
BAND 1	9.768	14.133	-4.365
BAND 2	1.653	1.561	0.092
BAND 3	-9.770	-49.014	39.244
BAND 4	-1.188	19.685	-20.874

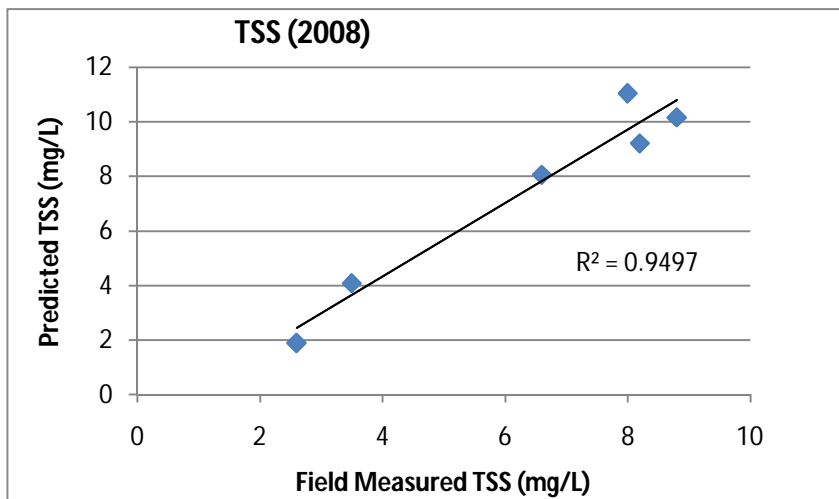
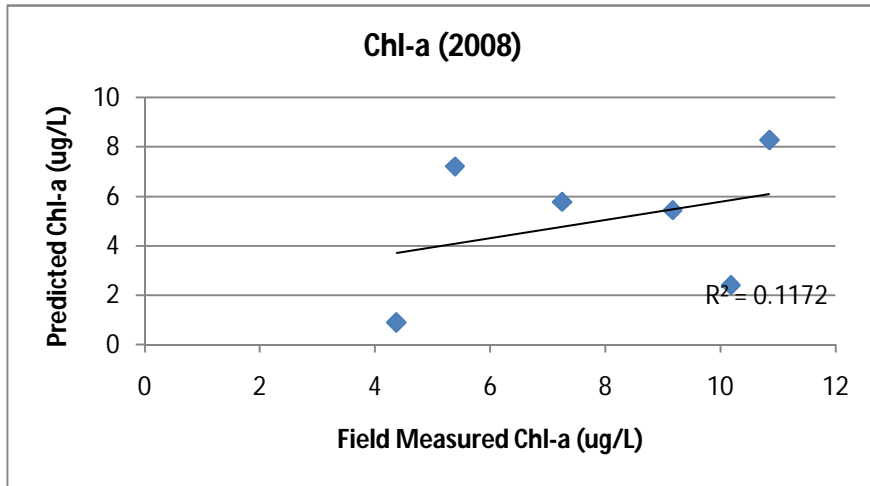
Appendix 7: Water Quality Parameter Model Performances based on the Jackknife Resampling Method (2007-2008).



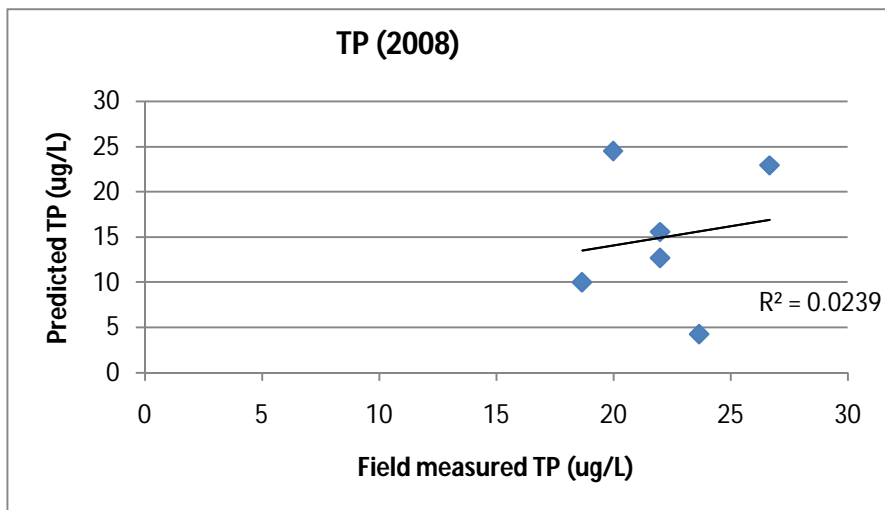
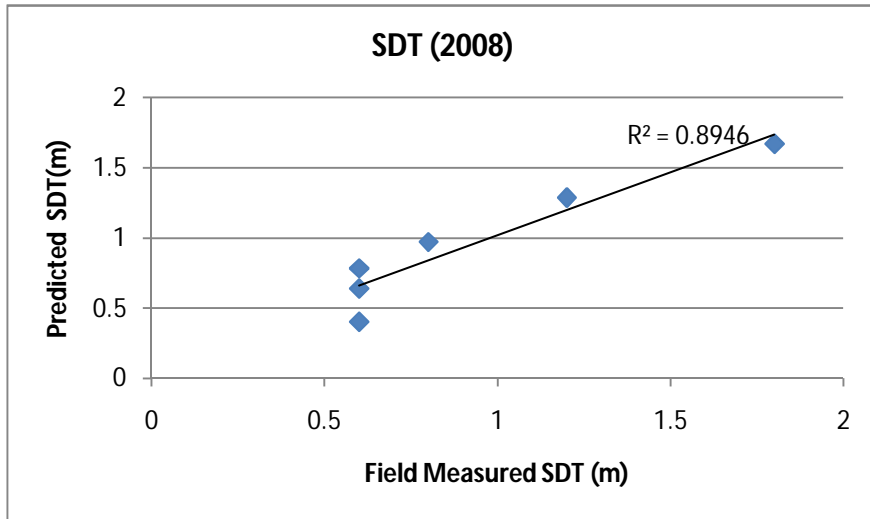
Appendix 7 continued



Appendix 7 continued



Appendix 7 continued



BIBLIOGRAPHY

Alparslan E, Yüce H., Erkan B., Nan S., Erg S., Saatçılar, R. (2006), 'Multi-Criteria Analysis of Landslide Susceptibility in the Area between Büyükçekmece and Küçükçekmece Lakes of Istanbul City Using Remote Sensing and GIS', in *Proceedings of the 4 th GIS Days in Turkey*, Fatih University, 13-16 September, 2006, Istanbul.

Barnes, K.B., Morgan J.M. III, Roberge, M.C. (2001), *Impervious surfaces and the quality of natural and built environments*, Towson, Maryland: Center for Geographic Information Services, Towson University, <http://pages.towson.edu/morgan/files/Impervious.pdf>. (12 May 2010).

Blokhuis, W.A., (1993). "Vertisols in the central clay plain of the Sudan" in R. Lal, (ed.), *Encyclopedia of Soil Science: Vol. 2*, Boca Raton, FL: Taylor and Francis, pp.1850.

Brando, V. E. and Dekker, A. G. (2003), 'Satellite hyperspectral remote sensing for estimating estuarine and coastal water quality'. *IEEE Transaction on Geoscience and Remote Sensing* 41:1378–1387

Brivio P.A., Giardino C., and Zilioli E. (2001), "Validation of satellite data for quality assurance in lake monitoring applications", *Science of the Total Environment*, 268 (1-3), pp. 3-18.

Brown, R.B. (2003), "Soils and Septic. Systems" *Fact Sheet SL-118*, University of Florida Cooperative Extension Service, <http://edis.ifas.ufl.edu/ss114>. (28 November, 2009).

Budhiman, S., Hobma, T.W. and Vekerdy, Z. (2004), Remote sensing for mapping TSM concentration in Mahakam delta: an analytical approach. 13th OMISAR Workshop on validation and application of satellite data for marine resources conservation, Kuta, Bali, Indonesia, 5-6 October 2004, pp.14.

Bukata, R.P., (2005), *Satellite Monitoring of Inland and Coastal Water Quality: Retrospection, Introspection, Future Directions*, Boca Raton, FL; London: Taylor & Francis.

Carlson, R.E. and J. Simpson. (1996), *A Coordinator's Guide to Volunteer Lake Monitoring Methods*, North American Lake Management Society. pp. 96, <http://dipin.kent.edu/Phosphorus.htm> (12december 2009).

Carpenter SR, Caraco NF, Correll DL, Howarth RW, Sharpley AN, Smith C.H. (1998), "Nonpoint pollution of surface waters with phosphorus and nitrogen", *Ecological Applications*, 8, 559–568.

Carr, James R. (2002), *Data visualization in the geological sciences*, Upper Saddle River, N.J: Prentice Hall, pp. 267.

Cincotta, Eric J. (1997), Atmospheric correction considerations of remotely sensed coastal waters, (M. Sc. Thesis, State University of New York, 1997). *ProQuest UMI Dissertation Publishing*.

Coppin, P. R. and Bauer, M. E. (1996), Change detection in forest ecosystems with remote sensing digital imagery, *Remote Sensing Reviews*, Vol. 13. pp. 207-234.

De la Cretaz, A.L. and Barten, P.K., (2007), *Land Use Effects on Streamflow and Water Quality in the Northeastern United States*, CRC Press, Boca Raton, 2007, p 43.

Dekker AG, Peters S. W. M (1993), "The use of the Thematic Mapper for the analysis of eutrophic lakes: a case study in the Netherlands", *International Journal of Remote Sensing* 14: 799-821.

Dekker, A.G., (1993), "Detection of Optical Water Quality Parameters Eutrophic Waters by High Resolution Remote Sensing", (Doctoral Dissertation, Vrije University, 1993). Amsterdam: Vrije University, 1-240.

Dekker, A.G., Malthus, T.J., Seyhan, E. (1991), Quantitative modeling of inland water quality for high-resolution mss systems. *IEEE Transactions on Geoscience and Remote Sensing*, 29, pp. 89-95.

Dekker, A.G., Malthus, T.J., Goddijn, L.M. (1992), "Monitoring cyanobacteria in eutrophic waters using airborne imaging spectroscopy and multispectral remote sensing systems", in *Proceedings of Sixth Australasian Remote Sensing Conference*, Wellington, New Zealand, November 2-6, 1992; Vol.1, pp. 204-214.

Dekker, A.G., Malthus, TJ., and Goddijn, L.M. (1992), "Monitoring cyanobacteria in eutrophic waters using airborne imaging spectroscopy and multispectral remote sensing systems" *Proceedings 6th Australasian Remote Sensing Conference*, Vol. I, Wellington, New Zealand, 2-6 November 1992, pp. 204-214.

Demirci, A., McAdams, M.A., Alagha, O., & Karakuyu, M. (2006), "The relationship between land use change and water quality in Küçükçekmece Lake watershed" in A. Demirci, M. Karakuyu & M. A. McAdams (Eds.), *Proceedings of 4th gis days in Türkiye* (p. 27-35). Istanbul, 13-16 September.

Dodds, W.K. (2002), *Freshwater Ecology: Concepts and Environmental Applications*, San Diego, London: Academic Press, pp. 569.

Driggers, Ronald G. (ed.) (2003), *Encyclopedia of Optical Engineering: Vol.2*, New York: Marcel Dekker, pp. 1398.

Ekercin, S. (2007). Water Quality Retrievals from High Resolution IKONOS Multispectral Imagery: A Case Study In Istanbul, Turkey. *Water, Air and Soil Pollution*, (DOI 10.1007/s11270-007-9373-5) (SCI).

EPA, (1999), *Combined sewer overflows: guidance for monitoring and modeling*, Washington, D.C: Office of Water, *United States Environmental Protection Agency*, <http://www.epa.gov/npdes/pubs/chap01-cso.pdf> . (12 May 2010).

Erinç, S., (1980), “Jeokoloji Açısından İstanbul Yöresi”, *İst. Üniv. Coğrafya Enst. Dergisi*, sayı 23, İstanbul.

Flemming, D. (2003), IKONOS DN value conversion to planetary reflectance, Version 2.1, CRESS Project, University of Maryland.

Folgo A Batista, Maria T.; Colaeo, Alexandra C.; Capelo, Sofia G.; Branco de Mascarenhas, Jose M. (2003), “LANDSAT/IKONOS applied to water quality monitoring in south of Portugal Remote Sensing for Agriculture, Ecosystems, and Hydrology IV”, in Owe, Manfred; D'Urso, Guido; Toullos, Leonidas(eds), *Proceedings of the SPIE*, Volume 4879, pp. 373-378.

Fuller, L.M. and Minnerick R.J. (2007), “Predicting Water Quality by Relating Secchi-Disk Transparency and Chlorophyll a Measurements to Landsat Satellite Imagery for Michigan Inland Lakes, 2001–2006, U.S. *Geological Survey Fact Sheet* 2007-3022.

Fuller, L.M., Aichele, S. S., Minnerick, R.J. (2004), “Predicting Water Quality by Relating Secchi-Disk Transparency and Chlorophyll a Measurements to Satellite Imagery for Michigan Inland Lakes, August 2002, *USGS Scientific Investigations Report*, 5086, pp. iv, 25.

Geosystems (2006): Calibration Files in ATCOR- A Mystery? Germering, Germany, pp. 218, [http://www.geosystems.de/atcor/downloads/Calibration Files in ATCOR.pdf](http://www.geosystems.de/atcor/downloads/Calibration%20Files%20in%20ATCOR.pdf) (accessed 5 May. 2009).

Geosystems (2008): *ATCOR for IMAGINE 9.3. User Manual ATCOR 2 and ATCOR 3*. Germering, Germany, pp. 218.

Giardino C., Pepe M., Brivio P.A., Ghezzi P., Zilioli E. (2001), “Detecting chlorophyll, Secchi disk depth and surface temperature in a sub-alpine lake using Landsat imagery”, *Science of the Total Environment*, 268 (1-3), pp. 19-29.

Gibson, G., (2000), *Nutrient criteria technical guidance manual: lakes and reservoirs*, Washington, D.C: Office of Water, Office of Science and Technology, U.S. Environmental Protection Agency.

Gibson, Paul J. and Power, Clare H. (2000), *Introductory Remote Sensing: Digital Image Processing and Applications*, London: Routledge.

Gilbes-Santaella, Fernando (2008), Monitoring Nutrients Content in the San Juan Bay Estuary Using Hyperspectral Remote Sensing, Department of Geology, University of Puerto Rico, Mayaguez.

Gitelson, A., Garbuzov, G., Szilagyi, F., Mittenzwey, K-H., and Karnieli, A., (1993), "Quantitative Remote Sensing Methods for Real-time Monitoring Inland Water Quality", *Int. J. of Remote Sensing*, Vol. 14, pp. 1269-1295.

Goetz, S. J., D. Varlyguin, A. J. Smith, R. K. Wright, C. Jantz, J. Tringe, S. D. Prince, M. E. Mazzacato, and B. Melchoir (2004). "Application of multitemporal Landsat data to map and monitor land cover and land use change in the Chesapeake Bay watershed" in P. Smits and L. Bruzzone (ed.), *Analysis of Multi-temporal Remote Sensing Images*, Singapore: World Scientific Publishers, pp. 223-232.

Gray, J.R., Glysson, G.D., Turcios, L.M., and Schwarz, G.E., (2000), *Comparability of suspended-sediment concentration and total suspended solids data: U.S.Geological Water-Resources Investigation Report 00-4191*, 14 p.

Guan, X. (2009), Monitoring Lake Simcoe water quality using Landsat TM images (M.Sc. dissertation, University of Waterloo (Canada), 2009) *ProQuest UMI Dissertation Publishing*, AAT MR56055.

Gupta, Ravi P. (2003), *Remote sensing geology*, 2nd ed. Berlin, New York: Springer, pp.655.

Hakvoort H., de Haan J., Jordans R., Vos R., Peters S. and Rijkeboer, M. (2002), "Towards airborne remote sensing of water quality in the Netherlands: validation and error analysis", *ISPRS Journal of Photogrammetry and Remote Sensing* 57: 171-183.

Han, L. and Rundquist, D.C., 1997, "Comparison of NIR/Red ratio and first derivative of reflectance in estimating algal-chlorophyll concentration: a case study in a turbid reservoir", *Remote Sensing of Environment*, 62, pp. 253-261.

Holland, J.M. (2004), "The environmental consequences of adopting conservation tillage in Europe: reviewing the evidence. Agriculture", *Ecosystems and Environment*, 103:1-25.

Icelandic Meteorological Office, Wind speed classification, http://andvari.vedur.is/english/wind_eng.html? (20 May 2010).

ISKI, <http://havza.iski.gov.tr/Default2.aspx> , (29 April, 2010)

Islam, M. R., S. F. Begun, Y. Yamaguchi, and K. Ogawa. (2001), "Suspend sediments in the Ganges and Brahmaputra rivers in Bangladesh: observation from TM and AVHRR data", *Hydrological Processes*, 15:493–509.

Istanbul Çevre ve Orman Mudurluğu , (2005), *Dogal Kaynaklar*, Çevre Durum Raporu.<http://www.istanbulcevor.gov.tr/pdf/cdr2005/03BDogalKaynaklar.pdf> (12december 2009).

Iwashita K., Kudoh K., Fujii H., Nishikawa H. (2004), "Satellite analysis for water flow of Lake Inbanuma," *Advances in Space Research*, 33 (3), pp. 284-289.

Jensen, J. R., (2007), *Remote Sensing of the Environment: An Earth Resource Perspective*, 2nd Edition, Upper Saddle River: Prentice-Hall, pp. 592.

Jerry C. Ritchie and Charles M. Cooper, (2001), "Remote Sensing Techniques for determining water quality: Applications toTMDLs" in TMDL Science Issues Conference, Water Environment Federation, Alexandria, VA 2001. pp. 367-374.

Jones, R.A., and Lee G.F.. (1979), "Septic tank wastewater disposal systems as phosphorus sources for surface waters", *Journal of the Water Pollution Control Federation* 51:2764-2775.

Ke-Sheng, Cheng, Tsu-Chiang Lei, Hui-Chung Yeh (1998), *Reservoir water quality monitoring using landsat TM images and indicator kriging*. GIS Development Proceedings, Asian Conference on Remote Sensing, November 16-27, 1998, Manila, Filipinas, <http://www.gisdevelopment.net/aars/acrs/1998/ts2/ts2004.asp> .(18 September 2009).

Kloiber, S.M., Brezonik, P.L., Olmanson, L.G. and Bauer, M.E. (2002), A procedure for regional lake water clarity assessment using Landsat multispectral data. *Remote Sens. Environ.* 82:38-47.

Lal, (ed.), (2006), *Encyclopedia of Soil Science: Vol. 2*, Boca Raton, FL: Taylor and Francis, pp.1850.

Lathrop, R. G. (1992), "Landsat Thematic Mapper monitoring of turbid inland water quality", *Photogrammetric Engineering and Remote Sensing*, 58, pp.465-470.

Liang, Shunlin, (2004), *Quantitative remote sensing of land surfaces*, Hoboken, New Jersey: John WileyandSons.

Lillesand, T.M, (2001). Combining satellite remote sensing and Volunteer Secchi disk measurement for Lake Transparency monitoring. Environmental Remote Sensing Center, University of Wisconsin, 1225 W Dayton st., Madison, WI53706 USA.

Loveland, T.R., Cochrane M.A., and Henebry G.M., (2008), "Landsat still contributing to environmental research", *Trends in Ecology and Evolution*, 23 (4), pp. 182-183.

McGarigal, Kevin, Sam Cushman, and Susan Stafford, (2002), *Multivariate Statistics for Wildlife and Ecology Research*, New York: Springer.

Melack, J. M. and Gastil, M. (2001), "Airborne remote sensing of chlorophyll distributions in Mono Lake, California", *Hydrobiologia* 466: 31–3828 :231-251.

Mittenzwey, K-H., Ullrich, S., Gitelson, A., Kondrat'ev, K., 1992, "Determination of Chlorophyll-a of Inland Waters on the Basis of Spectral Reflectance", *Limnology and Oceanography*, Vol. 37, No.1, pp. 147-149.

Mooney, Christopher Z., Duval, Robert D. (1993), *Bootstrapping: A Nonparametric Approach to Statistical Inference*. Sage University Papers Series No. 07-095. Newbury Park, CA : SAGE publications.

Moses, W. J., Gitelson A. A., Berdnikov S., and Povazhnyy, V. (2009), "Estimation of chlorophyll-a concentration in case II waters using MODIS and MERIS data-successes and challenges", *Environ. Res. Lett.*, 4 045005, pp.8.

Mueller, D.K., and Helsel, D.R., (1996), *Nutrients in the Nation's waters: Too much of a good thing?*, U.S. Geological Survey Circular 1136, 24 p.

Murphy, Sheila, (2005), *General Information on Dissolved Oxygen*, City of Boulder: USGS Water Quality Monitoring, <http://bcn.boulder.co.us/basin/data/BACT/info/DO.html> (27 May 2010).

National Research Council (U.S.) (1992), "Restoration of aquatic *eco*- systems: science, technology and public policy", *National Research Council*, Washington, D.C: Washington National Academy Press, pp. 544.

Nellis, M. D., Harrington, J. A., Wu, J.,(1998), " Remote sensing of temporal and spatial variations in pool size, suspended sediment, turbidity, and Secchi depth in Tuttle Creek Reservoir, Kansas: 1993", *Geomorphology* 21, 281-293 493–509.

OFCM, (1997), *Rawinsonde and Pibal Observations*, Federal Meteorological Handbook No. 3 - *Office of the Federal Coordinator for Meteorology*, Washington, DC <http://www.ofcm.gov/fmh3/text/chapter3.htm>.

Olmanson L.G., Bauer M.E., Brezonik P.L. (2008), "A 20 year Landsat water clarity census of Minnesota's 10,000 lakes". *Remote Sensing of Environment*, 112 (11), pp. 4086-4097.

Olmanson, L.G., Kloiber, S.M. Bauer, M.E. and Brezonik, P.L. (2002). Image processing protocol for regional assessment of lake water quality, Technical Report

146, Water Resources Center and Remote Sensing laboratory, University of Minnesota.

Ongley, Edwin D. (1996), *Control of water pollution from agriculture: FAO irrigation and drainage paper 55*, Rome: Food and Agriculture Organization of the United Nations, http://www.fao.org/docrep/W2598E/w2598e04.htm#chapter_1: introduction to agricultural water pollution. (12 May 2010).

Palluconi, F., Hoover, C., Alley, R., Jentoft-Nilsen, M., and Thompson, T. (1999), *An atmospheric correction method for ASTER thermal radiometry over land*, ASTER Standard Data Product, AST09.

Pattiaratchi, C., Lavery, P., Wyllie, A. and Hick, P., (1994), “Estimates of water quality in coastal waters using multi date Landsat Thematic Mapper data” *International Journal of Remote Sensing*, 15, p. 1571-1584.

Prepas EE, Charette T (2003), “Worldwide Eutrophication of Water Bodies: Causes, Concerns, Controls”. *Treatise on Geochemistry* 9:311-331.

Rao, C. R., Toutenburg, H., Shalabh and Christian H. (2008), *Linear Models and Generalizations, Least Squares and Alternatives*, Berlin, Heidelberg, Newyork: Springer, pp.563.

Rencz, Andrew N. (ed), (1999), *Remote Sensing for the Earth Sciences: Manual of Remote Sensing (3rd Edition) Vol. 3*, Canada: John Wiley and Sons, pp.728.

Ritchie, J.C. and Cooper. C.M., (2001), “Remote sensing of water quality: Application to TMDL”, in *TMDL Science Issues Conference*, Water Environment Federation, Alexandria, VA. pp. 367-375.

Ritchie, Jerry C., Paul V. Zimba, James H. Everitt (2003), “Remote Sensing Techniques to Assess Water Quality” *Photogrammetric Engineering and Remote Sensing*. 69 , pp. 695-704.

Sahu, Kali Charan (2008), *Textbook of remote sensing and geographical information systems*, New Delhi: Atlantic Publishers.

Sarıkaya Ö. Visali (2006), *Water Quality Analysis in the Golden Horn with the Help of IKONOS Imagery*, Unpublished M. Sc. Thesis, Istanbul Technical University.

Sass G.Z., Creed I.F., Bayley S.E., Devito K.J. (2007), “Understanding variation in trophic status of lakes on the Boreal Plain: A 20 year retrospective using Landsat TM imagery”, *Remote Sensing of Environment*, 109 (2), pp. 127-141.

Sawaya, K. E., Olmanson, L. G., Heinert, N. J., Brezonik, P. L., and Bauer, M. E., (2003). Extending satellite remote sensing to local scales: Land and water resource

monitoring using high resolution imagery, *Remote Sensing of Environment*, 88, pp.144-156.

Shao, Jun and Tu, Dongsheng (1995), *The Jackknife and Bootstrap*. Verlag: Springer.

Sharma, A.S., (2009), *Engineering Mathematics: Semester – III*, New Delhi: Discovery publishing House Pvt. Ltd., pp.279.

Sheng, T.C. (1990), *Watershed management field manual: Watershed survey and planning*, FAO Conservation Guide 13/6, Rome: Food and Agriculture Organization of the United Nations.

Shippert, P., (2004), "Why use hyperspectral imagery?" *Photogramm, Eng. Remote Sens.* 70 , pp. 377–396.

Singer, Arieh, (2007), *The soils of Israel*, Verlag:Springer, pp.306

Sullivan, P. (2004), Sustainable Soil management. Soil Systems Guide. ATTRA. <http://attra.ncat.org/attra-pub/PDF/soilmgmt.pdf>

SWCC (Soil and Water Conservation Committee, (2009), Alabama Handbook for Erosion Control, Sediment Control and Stormwater Management on Construction Sites and Urban Areas, Alabama.

UNEP (1995), Land Cover Assesment and Monitoring Training Manual, www.rrcap.unep.org/lc/cd/html/training/trainingmanual.doc, (25 November 2009).

UNESCO, (1999), "Applications of Satellite and Airborne Image Date to Coastal Management", *Coastal region and small island papers 4*, Paris: UNESCO, pp. VI + 185, <http://unesdoc.unesco.org/images/0011/001164/116472e.pdf>. (15 September, 2009).

Virmani, S.M., (1988), "Agroclimatology of the Vertisols and vertic soil areas of Africa", *International Crops Research Institute for the Semi-Arid Tropics (ICRISAT)*. <http://www.ilri.org/InfoServ/Webpub/Fulldocs/X5493e/x5493e04.htm>. (5May 2010).

Warner, Timothy A, Foody, Giles M., and Nellis, M Duane (ed.) (2009), *The SAGE Handbook of Remote Sensing*, London: SAGE publication Ltd.

Wells, M.R. (1988), *Assessment of Water erosion risk in Land capability studies: Swan Coastal Plains and Darling Range*, Technical Report 73, Western Australia: Division of Resource Management.

Westmoreland, Sally J. (2001), Radiometric Correction of Multisensor Imagery (Doctoral Dissertation, University of California Santa Barbara San Diego State University). *ProQuest UMI Dissertation Publishing*.

Whipple, William (1994), *New perspectives in water supply*, Boca Raton: *Lewis Publishers*.

Yang, Min-Der, Merry Carolyn J., Sykes Robert M. (1996), *Adaptive Short Term Water Quality Forecasts Using Remote Sensing and GI*, Virginia Water Resources Research Center Symposium Proceedings, September 22 - 26, 1996, Fort Lauderdale Florida , pp 109 – 118.

Yu, Ting (2005). Utility of remote sensing data in retrieval of water quality constituent's concentrations in coastal water of New Jersey. (Ph.D. dissertation, New Jersey Institute of Technology, 2005). *ProQuest UMI Dissertation Publishing*, AAT 3221750.

Zhang, Bo, (2008), *Data mining, GIS and Remote Sensing: Application in Wetland Hydrological Investigation* (Doctoral Dissertation, Ohio State University, 2008). *ProQuest UMI Dissertation Publishing*.

Zink, Norah E. (1939), "Dry-Farming Regions in Utah", *Clark University: Economic Geography*, Vol. 15, No. 4, pp. 421-431.